TECHNICAL UNIVERSITY OF LIBEREC
Faculty of Textile Engineering

FUNCTIONAL PROPERTIES OF SUPERHYDROPHOBIC TEXTILES

Muhammad Zaman Khan, M.Sc.

SUMMARY OF THE THESIS

Title of the thesis:	Functional Properties of Superhydrophobic Textiles
Author:	Muhammad Zaman Khan, M.Sc.
Field of study:	Textile Technics and Materials Engineering
Mode of study:	Full time
Department:	Material Engineering
Supervisor:	Prof. Ing. Jakub Wiener, Ph.D.

Committee for defense of the dissertation:

Chairman:	
prof. RNDr. Oldřich Jirsák, CSc.	FT TUL, Department of Nonwovens and Nanofibrous Materials
Vice-chairman:	
prof. Ing. Luboš Hes, DrSc., Dr.h.c.	FT TUL, Department of Textile Evaluation
prof. Dr. Ing. Miroslav Černík, CSc. (opponent)	CxI TUL, The Institute for Nanomaterials, Advanced Technologies and Innovation
doc. Ing. Vladimír Bajzík, Ph.D.	FT TUL, Department of Textile Evaluation
doc. Ing. Ladislav Burgert, CSc.	University of Pardubice, Faculty of Chemical Technology
doc. RNDr. Miroslav Šulc, Ph.D.	FP TUL, Department of Physics
Ing. Michal Černý, Ph.D. (opponent)	University of Pardubice, Faculty of Chemical Technology
Ing. Jana Šašková, Ph.D.	FT TUL, Department of Material Engineering
Ing. Blanka Tomková, Ph.D.	FT TUL, Department of Material Engineering

The dissertation is available at the Dean's Office FT TUL.

Liberec 2021

ABSTRACT

Over the last decades, researchers have been working to mimic the nature by inducing superhydrophobic properties into a variety of material surfaces so that they exhibit non-wetting properties. Many diverse applications have been found in the fields, such as space, defense, automotive, biomedical applications and engineering, sensors, apparels, and so on. This dissertation is about the development of superhydrophobic surfaces by inexpensive, simple and eco-friendly techniques with added functionalities (i.e. UV protection, Self-cleaning, Oil/Water separation, etc.) by deposition of fly ash, TiO_2 and ZnO particles.

The first study proposed simple and low-cost approach for improvement in UV protection and superhydrophobic properties of cotton fabrics by coating of mechanically activated fly ash particles. The maximum UV blocking was observed for 3 wt% fly ash, where UV transmittance decreased from 14.19% of untreated fabric to 0.11% of coated fabric. After subsequent treatment of Trimethoxy(octadecyl)silane (OTMS) on fly ash coated fabrics, the water contact angle was increased to 143^o, 147^o and 153^o for fly ash concentration of 1, 2 and 3 wt% respectively. From Cassie-Baxter theories, the unwetted fraction of air pockets were estimated to be 43%, 55% and 67% respectively for 1, 2 and 3 wt% of fly ash particles. Furthermore, the coated fabrics showed great potentials for separation of floating oil layer, underwater oil droplet or oil/water mixture. The separation efficiency of 98%, 96%, 97% and 95% was obtained for selected model oils toluene, n-hexane, chloroform and petrol ether, respectively.

In second study, the growth of 3D shaped TiO_2 flower particles on surface of polyester fabrics using two step approaches of sol–gel technology and hydrothermal method was successfully achieved. The scanning electron microscopy, EDS analysis, Raman spectroscopy, and X-ray diffraction techniques were employed to study the effect of Titanium isopropoxide (TTIP) concentration on the growth of flower-like TiO_2 microstructures. Atomic force microscopy (AFM) was carried out to evaluate the surface topography and roughness. Later, the layer of Trimethoxy(octadecyl)silane was applied on TiO_2 coated polyester fabrics to fabricate the self-cleaning textiles. The physical self-cleaning properties were examined based on superhydrophobicity and contact angle measurements where maximum static contact angle of 160.1^o and minimum roll off angle of 3^o was found for 2 mL TTIP dose. The degradation of methyl orange dyes under UV light irradiation was observed to confirm the photocatalytic chemical self-cleaning behavior, where the samples coated with 2 mL TTIP decolorized the dye solution in 150 min, whereas the samples coated with 1 mL and 1.5 mL TTIP took almost 300 and 210 min respectively.

In third study, a novel microwave hydrothermal method was employed on cotton fabrics to develop superhydrophobic surface by rapid synthesis of aligned ZnO nanorods on surface of the cotton fabric. Two step approaches was used for the growth of ZnO nanorods. First, cotton fabric was coated by seed layer of ZnO nanocrystals synthesized using microwave-assisted sol gel method. Secondly, ZnO nanorods were grown rapidly on the seeded cotton fabrics by microwave hydrothermal method. At last, layer of non-fluorinated silane was applied on as-grown nanorods to fabricate a superhydrophobic surface. The non-fluorinated silane was selected as this is less hazardous to skin compared to fluorinated silanes. The effect of zinc nitrate hexahydrate ($Zn(NO_3)_2 \cdot 6H_2O$) concentration, reaction time and microwave power on the growth of ZnO nanorods were investigated in detail using scanning electron microscopy (SEM). To study the structural properties of ZnO nanorods EDS analysis and X-ray diffraction (XRD) techniques were

used. Surface topography and roughness of the nanorods grown fabrics were studied using AFM. The superhydrophobic properties were examined based on contact angle and roll off angle measurements where maximum water contact angle of 170.2^{o} and minimum roll off angle of 1^{o} was found for 25 mM zinc nitrate hexahydrate ($Zn(NO_3)_2 \cdot 6H_2O$) concentration. The physical self-cleaning property was examined by using methyl orange dye as debris particles. The ZnO-OTMS coated fabrics were evaluated for superhydrophobic durability against mechanical abrasion, laundering, chemical and UV action. Moreover, the ZnO-OTMS coated fabrics showed excellent potentials for separation of floating and underwater oil layers or oil in water mixture. The oil in water separation efficiency of 99%, 98%, 98% and 96% was obtained for chloroform/water, n-hexane/water, petro ether/water and toluene/water, respectively.

Keywords: Fly ash particles; Superhydrophobicity; UV protection; Roughness; Oil water separation, TiO_2 nanoflowers; Physical self-cleaning; Chemical self-cleaning, ZnO nanorods; Microwave hydrothermal synthesis; Contact angle

ABSTRAKT

V posledních desetiletích se vědci snaží napodobovat přírodu tak, že připravují super hydrofobní povrchy různých materiálů, které mají nesmáčivé projevy. Tyto materiály nacházejí mnoho různých aplikací v řadě oborů a výrobků. Příkladem jsou kosmická technika, vojenský a automobilový průmysl, biomedicínské obory a strojírenství, čidla, speciální oděvy atd. Tato disertační práce se zabývá vývojem superhydrofobních povrchů s multifunkčními projevy (tj. UV ochrana, samočištění, separace olej / voda atd.) pomocí levných, jednoduchých a ekologicky orientovaných technik. Je využito ukládání částic popílku, strukturovaných nanočástic TiO_2 a ZnO s následnou silanizací.

V první studii je navržen jednoduchý a levný postup ke zlepšení ochrany proti UV záření a získání superhydrofobních vlastností bavlněných tkanin povrchovým nánosem mechanicky aktivovaných částic popílku. Maximální UV blokování bylo pozorováno pro 3 hmotnostní % popílku, kde propustnost UV klesla ze 14,19% pro neošetřené textilie na 0,11% pro upravené textilie. Po následné silanizaci pomocí trimethoxy (oktadecyl) silanu (OTMS) byl kontaktní úhel pro vodu zvýšen na 143^o, 147^o respektive 153^o pro koncentrace 1, 2 a 3 hmotnostní % popílku. Z teorie Cassie-Baxtera byl odhadnut podíl nesmočených vzduchových prostor (kapes) 43%, 55% a 67% pro 1, 2 a 3 hmotnostní % popílku. Kromě toho upravené textilie umožňovaly oddělení olejové vrstvy, kapiček oleje ve vodě nebo směsi oleje a vody. Účinnost separace 98%, 96%, 97% a 95% byla získána pro vybrané modelové oleje, toluen, n-hexan, chloroform a petroléter.

Ve druhé studii byl realizován růst částic TiO_2 tvaru nano květin na povrchu polyesterových tkanin pomocí dvou stupňového procesu sol-gel a hydrotermálního působení. Ke studiu účinku izopropoxidu titanu (TTIP) byly použity skenovací elektronová mikroskopie, EDS analýza, Ramanova spektroskopie a rentgenová difrakce. Pro vyhodnocení topografie povrchu a drsnosti byla použita mikroskopie AFM. Polyesterové textilie s nánosem TiO_2 tvaru nano květin byly následně silanizovány pomocí trimetoxy (oktadecyl) silanu s cílem přípravy samočistících textilií. Fyzikální samočisticí schopnosti byly zkoumány na základě měření superhydrofobicity pomocí kontaktního úhlu. Pro dávku 2 ml TTIP byl nalezen maximální statický kontaktní úhel 160,1° a minimální úhel skoulení kapky (roll off) 3^o. Pro potvrzení fotokatalytického chemického samočisticího chování byla hodnocena rychlost degradace barviva Metyl-oranž na upravených vzorcích při ozáření ultrafialovým světlem. U vzorku, kde byly pro růst TiO_2 nanočástic použity 2 ml TTIP došlo odbarvení za 150 minut, zatímco u vzorků, kde bylo použito 1 ml a 1,5 ml TTIP došlo k odbarvení po 300 a 210 min.

Ve třetí studii byla použita nová mikrovlnná hydrotermální metoda rychlé tvorby uspořádaných nano tyčinek ZnO pro vytvoření superhydrofobního povrchu na bavlněných tkaninách. Pro růst nano tyčinek ZnO byly použity dva kroky. Nejprve byla bavlněná tkanina potažena zárodečnou vrstvou nanokrystalů ZnO syntetizovaných metodou sol-gel s využitím mikrovlnného ohřevu. Růst nano tyčinek ZnO byl realizován na zárodečné povrchové vrstvě bavlněných tkanin mikrovlnnou hydrotermální metodou. Následně byla provedena silanizace pomocí prekurzoru neobsahujícího fluor, tak aby byl vytvořen superhydrofobní povrch. Vliv koncentrace hexahydrátu dusičnanu zinečnatého (Zn $(NO_3)_2$, $6H_20$), reakční doby a mikrovlnné energie na růst nano tyčinek ZnO byl podrobně zkoumán pomocí skenovací elektronové mikroskopie (SEM). Ke studiu strukturních vlastností nano tyčinek ZnO byly použity EDS analýza a rentgenové difrakce (XRD). Povrchová topografie a drsnost textilií obsahujících nano tyčinky ZnO byla studována pomocí AFM. Superhydrofobní vlastnosti byly zkoumány na základě měření kontaktního úhlu a měření

úhlu náběhu. Byl nalezen maximální kontaktní úhel vody 170,2° a minimální úhel skoulení kapky 1^{o} pro koncentraci hexahydrátu dusičnanu zinečnatého ($Zn(NO_3)_2.6H2O$) 25 mM. Fyzikální samočisticí vlastnosti byly zkoumány pomocí částic nečistot simulovaných barvivem Metyl-oranž. Byly hodnoceny také odolnosti proti mechanickému oděru, praní, chemickému a UV působení. Bylo také nalezeno, že upravené textilie mají schopnost separace různých směsí vody a olejů. Účinnost separace oleje od vody 99%, 98%, 98% a 96% byla získána pro směs chloroform/voda, n-hexan/voda, petroléter/voda a toluen/voda.

Klíčová slova: Částice popílku; superhydrofobicita; ochrana proti UV záření; drsnost; oddělení oleje a vody; nano květiny TiO_2; fyzikální samočištění; chemické samočištění; nano tyčinky ZnO; mikrovlnná hydrotermální syntéza; kontaktní úhel

TABLE OF CONTENTS

1. Introduction

The superhydrophobicity of solid surfaces has been investigated with considerable attention over the past few years due to the increased demands of impermeable textiles, self-cleaning coatings, non-adhesive coatings, microfluidic devices, biosensors and outdoor antennas [1], [2]. Based on superhydrophobic species existing in nature (e.g. lotus leaves, butterfly wings, and water strider legs), surface roughness and low surface energy of materials can be considered as the two important factors to obtain superhydrophobic surfaces [3]. The self-cleaning textiles also hold great promise for military applications where there is a lack of time for laundering at severe conditions, and in business life when clothes get stained accidentally [4]. Currently, there are two main concepts used in developing self-cleaning textiles [5]. The first concept (physical self-cleaning) is based on the superhydrophobic approach where water droplets attain the spherical shape and then they roll off the surface carrying away the dirt particles [6]. The second concept (chemical self-cleaning) is based on the process of photo-catalysis where the dirt/stain molecules break down to simpler species (such as CO_2 and water) on exposure to light [7]. For physical self-cleaning, the surface roughness and low surface energy of materials are the two important factors to control the wettability of a surface and to obtain water contact angles greater than 150^o [3]. As an inspiration from nature scientists have fabricated superhydrophobic textiles by creating surface roughness in combination with low surface energy materials such as organic silanes, fluorinated silanes, alkyl amines and silicates [8]–[10]. For chemical self-cleaning, polycrystalline semiconductor oxides have been applied in the form of nano-coatings, leading to the successful development of a number of UV-active self-cleaning textiles [11].

In early 90s, the researchers started to explore the natural surfaces having superhydrophobic and self-cleaning properties. These natural surfaces include the lotus plant, rice and Colocasia esculenta etc. In 1963, DuPont introduced its fluorochemical based product for treating fabrics which was called Zepel fabric fluoridizer. After treatment, the fabric exhibited water and oil repellency. The first time lotus effect mechanism was studied and reported by Barthlott and Neinhuis in 1997 [12]. During this study, it was found that self-cleaning property is due to presence of hierarchical rough surface structure of plant leaves. Since then, this type of self-cleaning of plant leaves is called lotus effect.

During last two decade research interests on superhydrophobicity and self-cleaning surfaces have grown tremendously. Such superhydrophobic surfaces have many applications such a self-cleaning, anti-corrosion, anti-fogging/frosting, oil/water separation, and anti-bio adhesion applications. Superhydrophobic textiles having oil in water separation ability are valuable to overcome the problems caused by oil spillage accidents. Furthermore, many other novel multifunctional applications for superhydrophobic surfaces have started to gain attention, like UV-protection, photocatalytic activity, anti-bacterial, EMI shielding, flame-retardant and anti-adhesion [13]. In order to defend other properties against damage, it has become an increasing trend to integrate the superhydrophobicity with additional functionalities.

Thus, attention should be paid to research on environmentally friendly preparation methods, as well as durability and mechanical stability of the textiles. In this context, this research work is focused on the development of superhydrophobic textiles with added functionalities (i.e. UV protection, Self-cleaning, Oil/Water separation) by deposition of fly ash, TiO_2 and ZnO nanostructures.

2. Purpose and the aim of the thesis

The overall objectives of this research work are to develop the superhydrophobic textiles with added functionalities (i.e. UV protection, Self-cleaning, Oil/Water separation, etc.) by deposition of fly ash, TiO_2 and ZnO nanostructures. The main purpose and aim of the thesis is described below.

2.1. Superhydrophobic fabrics coated with fly ash and OTMS

Aim of first study was to use mechanically activated fly ash to create effective and durable coating on cotton fiber surface for enhancing superhydrophobicity, UV protection, physical self-cleaning and oil in water separation. To the best of the author's knowledge, this is the first study on fly ash coated cotton fabrics. The coating of fly ash particles has never been studied for UV blocking properties of textiles despite their high refractive index and presence of metal oxide constituents in chemical composition.

2.2. Superhydrophobic fabrics coated with TiO_2 nanoflowers and OTMS

Aim of second study was to fabricate the polyester based self-cleaning textiles which are simultaneously superhydrophobic and photocatalytic. The 3D shaped TiO_2 flower particles grown on surface of polyester fabrics using two step approaches of sol–gel technology and hydrothermal method with subsequent silanization by Trimethoxy(octadecyl)silane (OTMS) were proposed as active layer. The flower-like TiO_2 hierarchical structure was proposed for obtaining excellent photocatalytic properties and inhibit defects of micron and nanometer structures due to their more abundant porous structure, larger specific surface area, lower density, better surface permeability, greater light-harvesting capacity, good light absorption efficiency, and appropriate refractive index [14].

2.3. Superhydrophobic fabrics coated with ZnO nanorods and OTMS

Aim of third study was to develop superhydrophobic cotton fabrics by using of a novel microwave hydrothermal method to grow vertically aligned ZnO nanorods on cotton fibers surfaces with subsequent silanization by Trimethoxy(octadecyl) silane (OTMS). This novel microwave hydrothermal method to grow ZnO nanorods is a simple, inexpensive, and time saving, low temperature and affective control over morphology. The study of effect of salt concentrations, reaction time and microwave power on the morphology of ZnO nanorods was proposed.

The specific objectives are as follow;

- Deposition of nanoparticles by different methods to achieve hierarchical surface roughness.
- Application of non-fluorinated silane (i.e. Trimethoxy(octadecyl)silane) to modify the surface chemistry.
- Characterization of surface morphology and topography of nanoparticle coated fabrics by different microscopy techniques.
- Evaluation of superhydrophobic properties from contact angle, sliding angle and contact angle hysteresis tests, and the validation of results by Cassie-Baxter model.
- Characterization of superhydrophobic durability against chemical and mechanical treatments.
- Evaluation of other essential properties, such as UV protection, Physical self-cleaning, Chemical self-cleaning, Oil-water separation and durability properties.

3. Overview of the current state of the problem

The superhydrophobic surfaces exhibits the water contact angles greater than 150° and roll-off angle less than 10°. Over the past decade, there have been many successful attempts at artificially reproducing the surface structures found on natural superhydrophobic surfaces. Currently, the most superhydrophobic surfaces are developed by using expensive, time consuming methods, precious equipment, high energy and less eco-friendly conditions. There are still many challenges on large scale fabrication of superhydrophobic surfaces by inexpensive, simple and eco-friendly techniques [15]–[18]. Moreover, other novel multifunctional applications for superhydrophobic textiles started to merge, including UV-blocking, photocatalytic, antibacterial, flame-retardant, anti-fogging/frosting, oil/water separation, and anti-bio adhesion. Among all properties, the integration of UV protection on superhydrophobic surfaces is of great concern in present work. This is because, the risks of UV radiations to induce acute and chronic illnesses, when they interact with skin, increased significantly in recent years [19]. Recently, numerous efforts have been made to simultaneously create superhydrophobic and photocatalytic surfaces which not only repel water but also decompose organic contaminates at the same time. However, the fabrication of superhydrophobic and photocatalytic surface is challenging because this surface either loses its superhydrophobicity upon irradiation with light or does not show a photocatalytic property [20].

Fabrication of superhydrophobic surfaces has been an area of active research since the mid-1990s. In general, different techniques that is used for the micro and nanostructure fabrication, such as lithography, etching, and deposition and self-assembly, has been utilized for producing superhydrophobic surfaces. There are two main requirements for the development of superhydrophobic surface, such as roughness of the surface and it should be hydrophobic (low surface energy). These two things lead to two methods for the fabrication of superhydrophobic surface: first, it is possible to make a rough surface from an initially hydrophobic material and secondly to modify a rough hydrophilic surface by modifying surface chemistry or by applying low surface energy material on it. Roughness is usually a more critical property than the low surface energy, since both moderately hydrophobic and very hydrophobic materials can exhibit similar wetting behavior when roughened [21]. Surface modification of the surface having roughness is carried out by using low surface energy materials such as fluorocarbon, organic silanes, fluorinated silanes, alkyl amines and silicates. In order to defend other properties against damage, it has become an increasing trend to integrate the superhydrophobicity with additional functionalities [22]. Several methods are reported for the development of superhydrophobic surfaces including hydrothermal technique, sol gel method, dip coating, electro-chemical method, layer-by-layer method, chemical vapor deposition, and spray coating [23]–[25].

In recent years, lot of research has been done to develop superhydrophobic textiles using nanoparticles of ZnO, TiO_2, and SiO_2, etc. Excellent UV protection was achieved by deposition of TiO_2 on polyester fabric [26]. TiO_2 and ZnO nanoparticles are also used for this purpose as they have good UV protection properties. They give protection by reflecting, scattering or absorbing harmful UV radiations of sun. The incorporation of TiO_2 nanoparticles by titania sol-gel coating can cause surface roughness for enhancing the superhydrophobicity of the fabric [27]. Carbon fabric was coated with silica nanoparticles to make it superhydrophobic [28]. Although TiO_2 or ZnO are widely used inorganic UV blockers, but they accelerate the photo damage of human skin due to high photocatalytic activity [29]. Therefore, the searches on safe UV shielding agents that possess superior shielding efficiency with poor photocatalytic property have become an urgent necessity. Fly ashes (FA) are aluminosilicate rich by-products generated in coal firing powder

plants. They are unique, non-toxic, chemically and physically stable, abundant and cheap, low density particles. In these circumstances, fly ash can be utilized as simple and low-cost approach for improvement in UV protection and superhydrophobic properties of cotton fabrics by coating of mechanically activated fly ash particles. Interestingly, fly ash particles have been reported to create micro/nanoscale roughness on the surface of fibers economically, however the researchers did not mention the additional benefits of fly ash coated fabrics [30]. There are still many challenges exist, like physical, chemical stability and cost of materials. These problems are needed to be solved before large scale production of these special surfaces. The development of highly robust superhydrophobic surfaces is important issue for future research.

4. Methods used, material studied

4.1. Materials

Fly ash was obtained from the city of Plzeň located in the Czech Republic with the help of SILO Transport organization. The fly ash was light gray in color with density of 2 g/cc. The main constituents of fly ash as determined by elemental analysis are 53.80% O, 20.25% Si, 14.27% Al, 4.72% Fe, 1.95% Ti, 1.84% Na, 1.06% Mg, 0.94 %Ca, 0.34% Zr, 0.25% K, 0.19% S, 0.16% Cu, 0.15% As, and 0.09% P. According to the composition, fly ash was classified in class-F category (ASTM C618) based on more than 70% total content of silica and alumina together. Titanium isopropoxide $Ti[OCH(CH_3)_2]_4$, Titanium butoxide $Ti(OBu)_4$, Hydrochloric acid, Caustic soda, Ethanol, Acetic acid, Zinc acetate dihydrate [$Zn(CH_3COO)_2.2H_2O$, ≥99% purity], Hexamethylenetetramine (HMTA, $C_6H_{12}N_4$, 99%) and OTMS (analytical grade) were purchased from Merck (Sigma Aldrich) and used as received. Zinc nitrate hexahydrate ($ZnN_2O_6 \cdot 6H_2O$, 99% pure) was obtained from Alfa Aesar. To investigate oil in water separation performance, four model oils of varying density (i.e. toluene, n-hexane, chloroform, petro ether) were used from laboratory. Plain woven bleached 100% cotton fabric and plain woven 100% polyester fabric was used as substrate to create superhydrophobic surfaces.

4.2. Superhydrophobic fabrics coated with fly ash and OTMS

4.2.1. Preparation of mechanically activated fly ash

Mechanical activation of fly ash was carried out using high-energy planetary ball mill of Fritsch Pulverisette 7 in a sintered corundum container of 80 ml capacity using zirconia balls of 10 mm diameter for the duration of 30 min. The ball mill was loaded with ball to fly ash weight ratio of 5:1. The rotation speed of the planet carrier was kept at 850 rpm. During milling, fly ash particles were subjected to a severe plastic deformation due to the repetitive compressive loads arising from the impacts between balls and fly ash. The milled fly ash particles were taken out to test particle size distribution on Malvern Zetasizer Nano based on dynamic light scattering principle. The deionized water was used as dispersion medium. The dispersion was ultrasonicated for 5 min under Bandelin ultrasonic probe before characterization. Refractive index of 1.55 was used for fly ash to calculate particle size. In addition, morphology of fly ash after ball milling was observed on Scanning electron microscope (SEM) TS5130-Tescan at 30 kV accelerated voltage.

4.2.2. Preparation of fly ash coated cotton fabrics

Mechanically activated fly ash particles were added at 1, 2 and 3 wt% concentration into distilled water and the dispersion was sonicated for 15 min using ultrasonic system (Bandelin Sonopuls HD 3200, 20 kHz, 200 W, 50% efficiency). Then, the fly ash dispersion was applied on bleached cotton

fabric through a dip-pad-dry-cure process. The fabric was immersed into the dispersion for 1 min, subsequently passed through a padder, dried at 80°C in a drying oven and finally cured at 120 °C for 3 min.

4.2.3. Hydrophobization of fly ash coated cotton fabrics

For fabrication of superhydrophobic surfaces, OTMS was applied on fly ash coated cotton fabrics to lower their surface energy. The OTMS has very long chain of carbon atoms which impart hydrophobicity. The OTMS (8%, w/w) was added drop wise into ethanol, and acetic acid was employed to promote the hydrolysis of OTMS by adjusting pH values in 4-5 range. The solution was stirred at room temperature for 45 min. The fly ash coated cotton fabrics were then immersed in hydrolyzed OTMS solution, dried in air and cured at 120 °C for 1 hr. One control sample was also prepared without any surface decoration of fly ash particles. Figure 1 shows the schematic of fabrication of superhydrophobic surfaces.

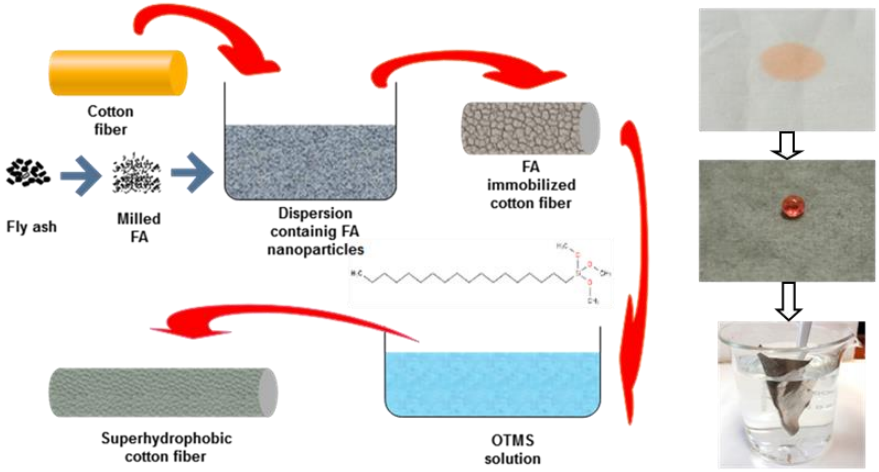

Figure 1. Fabrication of fly ash-OTMS coated superhydrophobic cotton fabric

4.3. Superhydrophobic fabrics coated with TiO_2 nanoflowers and OTMS

4.3.1. Synthesis of flower shaped TiO_2 particles on polyester fabric

At the beginning, the surface of polyester fabric was cleaned by petroleum ether for 2 hr at 60 °C in Soxhlet apparatus and later treated with 20 g/L caustic soda solution at 80 °C for 30 minutes. Then, the flower shaped TiO_2 particles were grown on surface of polyester fibers using two step approaches of sol–gel technology and hydrothermal method. In the first step, a semitransparent TiO_2 sol was formed by continuously stirring a mixed solution of Titanium butoxide (6 mL), ethanol (60 mL) and acetic acid (2 mL) for 3 h at 60 ^oC. The caustic soda treated polyester fabric was immersed in the prepared TiO_2 sol for 5 min, padded with a wet pickup of 70–80% and dried at 110 ^oC. This process was repeated 3 times and the samples were cured at 140 ^oC. In the second step, hydrothermal method was used to grow the flower shaped TiO_2 particles on the already TiO_2 seeded fabric. Here, different amounts of titanium isopropoxide were added drop wise into the aqueous hydrochloric acid solutions (i.e. 10 mL HCl and 60 mL distilled water), and the mixtures were stirred for 10 min until the solutions turned clear. The resulting solution was further transferred into 150-mL Teflon-lined stainless-steel autoclave and TiO_2 seeded polyester fabric was placed in it. The autoclave was placed in an oven for 1 h at 125 °C. Finally, the polyester fabric was removed from the autoclave, rinsed with deionized water and dried at room temperature.

4.3.2. Superhydrophobization of TiO_2 nanoflowers coated polyester fabrics

The OTMS was applied on TiO_2 coated polyester fabrics for fabrication of superhydrophobic surfaces by lowering the surface energy. The OTMS solution was prepared by addition of (8%, w/w) OTMS drop wise into ethanol and stirring it at room temperature for 45 min. The hydrolysis of OTMS was promoted by use of acetic acid and by adjusting pH values in 4-5 range. The polyester fabrics decorated with different concentrations of 3D shaped TiO_2 flowers were then immersed in hydrolyzed OTMS solution, dried in air and cured at 120 °C for 1 hr. One control sample was also prepared by just coating of OTMS alone and without any surface decoration of TiO_2 nanoflowers. The schematic of fabrication of superhydrophobic surfaces can be seen as continued process to decoration of TiO_2 flowers from Figure 2.

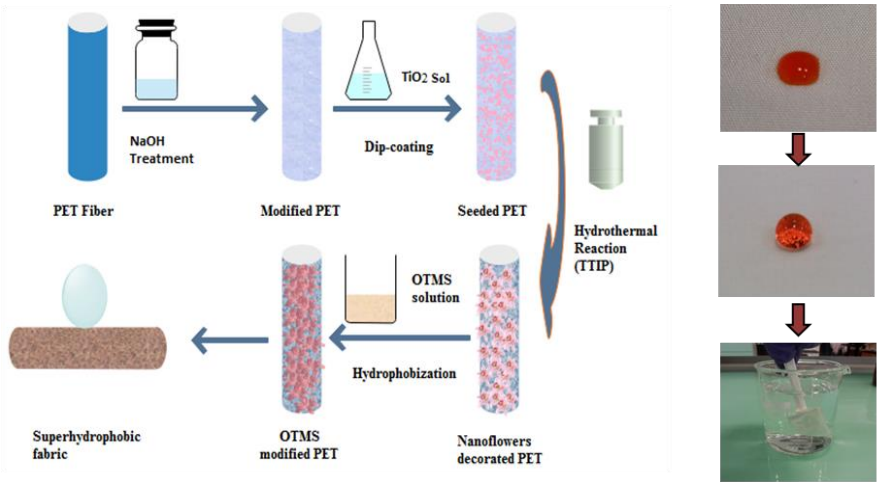

Figure 2. Schematic of deposition of TiO_2 flower shaped particles on polyester fabric

4.4. Superhydrophobic fabrics coated with ZnO nanorods and OTMS

4.4.1. Preparation of ZnO nanocrystals

Two step processes was used to grow ZnO nanorods on cotton fabric. In first step the Zinc oxide nanocrystals were prepared by microwave-assisted sol gel method. Zinc acetate dihydrate (25 mM) was dissolved in ethanol under stirring at room temperature followed by addition of sodium hydroxide (75 mM) in ethanol solution. Then the 50 mL resultant solution was transfer to Teflon reaction container and closed firmly. The reaction container was put into the microwave reactor (Magnum II reactor, 600 W, 2.45 GHz, ERTEC, Poland) and reaction was carried out at 60 °C (360 W) for 10 min. Finally, a transparent ZnO seed solution was obtained. The as-prepared ZnO nanocrystals seed solution was deposited onto the cotton fabric by dip-pad-cure process. The cotton fabric was dipped into solution, then dried at 110 °C and cured at 150 °C for 5 min in an oven to ensure ZnO nanocrystal particles adhere to cotton fiber surface.

4.4.2. Growth of nanorods

In second step, ZnO nanorods were grown on these seed layer deposited cotton fabrics through microwave hydrothermal synthesis. Equimolar aqueous solutions of zinc nitrate hexahydrate and hexamethylenetetramine (HMTA) were prepared by mixing 25 mL of each solution to make 50 mL solution. The cotton fabric seeded with ZnO nanocrystals and resultant solution was transferred to Teflon reaction container and container was put into the microwave reactor

(Magnum II reactor, 600 W, 2.45 GHz, ERTEC, Poland). In situ synthesis of ZnO nanorods on cotton fabric was carried out using microwave hydrothermal technique under various conditions. The effect of zinc nitrate hexahydrate concentration (10 mM, 25 mM, 50 mM, 75 mM, and 100 mM), reaction time (10 min, 20 min, 30 min) and microwave power (360 W, 420 W, 480 W) was studied in detail. After reaction, the samples were taken out and rinsed in deionized water for 3 times and dried at 100 °C for 10 min.

4.4.3. Superhydrophobic treatment of ZnO nanorods grown cotton fabrics

The OTMS was applied on ZnO nanorods coated cotton fabrics for development of superhydrophobic surfaces by lowering the surface energy. The OTMS solution (8%, w/w) was prepared by stirring at room temperature for 45 min. The ZnO nanorods coated cotton fabrics were then immersed in the OTMS solution, air dried and then cured at 120°C for 1 hr. One control sample was also prepared by coating of OTMS alone on cotton fabric. The schematic showing methods used for development of superhydrophobic cotton fabrics (see Figure 3).

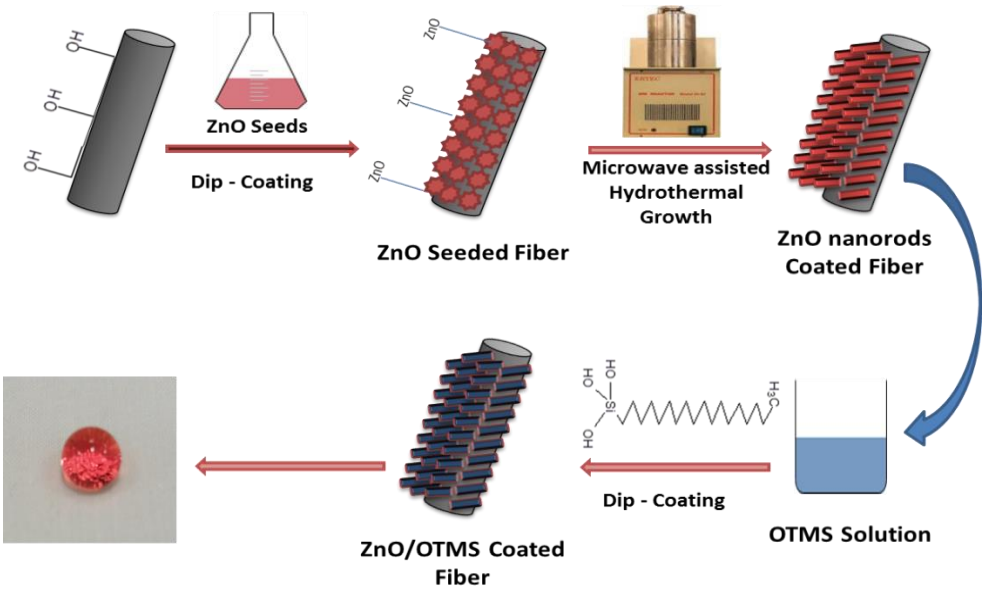

Figure 3. Shows the schematic of development of superhydrophobic cotton fabrics

4.5. Characterization of surface morphology of coated fabrics

4.5.1. SEM and EDS analysis

The scanning electron microscope (SEM) of TS5130 Vega Tescan was employed to observe the surface morphology of coated fabrics at 30 kV acceleration voltages. The gold sputtering was performed to develop the conductive layer on surface of samples before SEM analysis. For better resolution, the surface structure of coated samples was also seen under the field emission scanning electron microscope of Zeiss Ultra Plus at an accelerating voltage 2 kV equipped with an Energy Dispersive X-ray spectrometer Oxford X-max 20.

4.5.2. Raman spectroscopy

For characterization of crystal phases, the Raman spectra were recorded by DXR Raman Microscope (Thermo Scientific, USA) with 532 nm laser, grating 900 lines/mm in spectral range of 3500-50 cm^{-1} and objective Olympus LMPlanFL 10x and 50x. The 25 and 50 μm slit spectrograph aperture was used with 0.9 to 5.0 mW level of laser power, 1 sec exposure time and 50 exposures.

4.5.3. X-Ray diffraction (XRD) analysis

The crystalline structure of material was studied on X-Ray diffraction (XRD) analysis of PAN analytical X'pert PRO equipment. The XRD analysis was performed with a diffractometer equipped with a conventional X-ray tube Cu kα1 radiation (**λ**=1.5406 Å) power condition (40 KV/30 mA). The XRD pattern was measured in the 2θ range of 20-70 with the step size of 0.02.

4.5.4. Atomic force microscopy (AFM) analysis

In this study, NanoWizard 3 NanoScience AFM from JPK Instruments was used in non-contact mode to determine the surface roughness and to observe the topography of the coated samples. For all samples, at least three topographic images were obtained and surface roughness was calculated. The software calculates the surface roughness average (Ra) directly from AFM signals using the Equation (1).

$$R_a = \frac{1}{L}\int_0^L |Z(x)|\ dx \tag{1}$$

Where Z(x) is the function that describes the surface profile analyzed in terms of height (Z) and position (x) of the sample over the evaluation length (L).

4.6. Characterization of UV protection properties

UV protection behavior of the coated fabrics was determined by measuring percentage transmission of UV radiations on UV-vis-NIR Spectrophotometer (UV-3101PC) as per AATCC 183-2000 standard. The samples were conditioned for 4 hours at 21 ± 1 °C temperature and 65 ± 2 % relative humidity. For each sample, four measurements were performed and the average of scans was taken to calculate the UPF factor from Equation (2).

$$UPF = \frac{\sum_{280nm}^{400nm} E_\lambda S_\lambda \Delta_\lambda}{\sum_{280nm}^{400nm} E_\lambda S_\lambda T_\lambda \Delta_\lambda} \tag{2}$$

Where S_λ is the solar spectral irradiance, E_λ is the relative erythemal spectral response, T_λ is the average spectral transmittance of the sample and Δ_λ is the measured wavelength interval in nanometres.

4.7. Characterization of physical properties

The uptake (i.e. add on percentage) of coated fabric was calculated using the Equation (3).

$$Add\ on\ (\%) = \frac{w_f - w_i}{w_i} \times 100 \tag{3}$$

Where w_i is weight of fabric before coating and w_f is weight of fabric after coating.

Furthermore, the coated fabrics were investigated for the comfort properties based on the measurements of stiffness from the TH-7 instrument which is similar to standard Kawabata KES-FB 2 device used for testing of low stress mechanical properties [31].

4.8. Characterization of superhydrophobicity of coated fabrics

4.8.1. Contact angle measurement

Surface energy evaluation system of Advex instrument was employed to measure the contact angle of the coated fabrics. It is a computer-aided instrument which uses the sessile drop method to calculate the contact angle between liquid and solid. . Six measurements were made on each sample with 5 μL of water droplet and average contact angle was determined.

4.8.2. Roll off angle measurement

The roll off angle was measured by using a custom-made device, which can measure the roll off angle with an accuracy of 1°. The spirit level was used to balance the apparatus on table. Sample was fixed on device and 5 μL water droplet was dropped from a syringe on the fabric. Then, the plate was inclined slowly (1°), until the droplet started to move. On each sample, six measurements were made and mean value was taken.

4.8.3. Contact angle hysteresis

The advancing contact angle was measured when needle was brought in close proximity to the sample surface, and the deionized water was pumped until the drop reached a size of approximately 25 μL. Subsequently, the receding angle was measured when the liquid was pumped in at the same rate until the detached drop from the needle or all of the liquid returned to the syringe. Then, the contact angle hysteresis was estimated from the difference between the advancing and the receding contact angles. The test was repeated three times for each specimen at different locations.

4.8.4. Durability of contact angle

The mechanical abrasion durability of the coated fabrics was studied from the sand paper test. The coated fabric was dragged against sand paper surface after putting 100 g load on the top of the sample and the change in contact angle after 20 abrasion cycles was examined [32]–[34]. Further, the washing durability was examined by measuring the contact angle after five laundering cycles according to ISO 105 C06 (B1M) standard (4 g L^{-1} detergent, 60 °C temperature and 45 min time). The chemical durability was evaluated by measuring the contact angle after immersing the coated fabrics into acidic (pH=1) and alkaline (pH=13) solutions for the duration of 24 h. For evaluation of UV durability, the coated cotton fabrics were placed under ultraviolet lamp Philips TL 6W UV tubes (315-400 nm) for 24 h and then their contact angle was measured. The durability against a jet of water was also studied by observation of the bouncing of water droplets. A jet of water was impacted on the fabric surface with speed of 3 m/s by a syringe kept at 4 cm above the sample with an angle of 45° for 1 min, and the bouncing of water droplets was captured in the high-speed camera (Olympus, *i-SPEED 3*) at 5000 frame s^{-1}.

4.9. Characterization of self-cleaning properties of coated fabrics

4.9.1. Physical self-cleaning

The 0.5 g methyl orange dye was used as contaminant and it was randomly sprinkled over the coated fabric surface. Then, the physical self-cleaning property was studied by rolling the water over the dye contaminated surfaces. The directed movement of water droplets was observed in digital camera by introduction of water droplets at an angle of 45° on the coated fabric surface using micropipette.

4.9.2. Chemical self-cleaning

As the coated fabrics were superhydrophobic in nature, therefore they were not immersed directly in aqueous solution of methyl orange dye. The superhydrophobic fabrics were first soaked in acetone and then immersed in dye solution for the chemical self-cleaning behavior using two different experiments (i.e. stain degradation and solution discoloration). For stain degradation, the dyed samples were irradiated under the UV light of Philips TL 6W UV tubes (315-400 nm) and the stain degradation performance was evaluated as a function of exposure time to UV light. Later, the fabric surfaces discolored after the tests were scanned with 300 dpi and the scanned images were analyzed to calculate the color intensity by Image J software [35]. For solution discoloration experiments, the coated samples with diameter 2.8 cm were placed in a beaker having 15 ml of methyl orange dye solution. This beaker was then placed below the light source Philips TL 6W UV tubes (315-400 nm) at a distance of 18 cm. To estimate the photo catalytic discoloration effect, an aliquot was removed from the solution after a pre-set time interval and its absorbance was measured at λ_{max} (485 nm) using UV-Vis Spectrophotometer (UV-1600PC).

4.10. Oil/water separation property of the coated fabrics

The coated superhydrophobic fabrics were tested for oil in water separation performance using four model oils of different densities (n-hexane, toluene, chloroform, petro ether) mixed in water (50% v/v). The coated fabric was placed on top of the small beaker which was mounted in another big beaker. When oil/water mixture was poured onto the surface of coated fabric, oil penetrated through the fabric into small beaker whereas water flowed into the big beaker. The oil/water separation efficiency (%) was calculated from the ratio of volume of oil remaining after separation to initial volume of oil mixed with water. For measurement of oil absorption capacity, the coated fabric samples were immersed in an oil/water mixture for 5 s, removed, and then weighed immediately. The oil absorption capacity (Q) of the fabric was calculated from weights measured at room temperature using Equation (4).

$$Q = \frac{(W_t - W_i)}{W_i} \times 100 \qquad (4)$$

Where W_t is the weight of the saturated coated fabrics after immersing in oil/water, and W_i is the weight of the fresh coated fabrics.

5. Summary of the results achieved

5.1. Superhydrophobic fabrics coated with fly ash and OTMS

5.1.1. Mechanical activation of fly ash

Figure 4 (a) shows the particle size distribution of fly ash after 30 min of dry milling. It can be seen that the size of fly ash particles was greatly reduced after the grinding. The unmilled fly ash with mean particle diameter of 3547 nm was converted to smaller particles of mean below 1000 nm diameter. When milling was continued for longer time, the temperature of milling container was increased. This resulted in sticking of fly ash layer on surface of milling container, and therefore further grinding of fly ash was not continued. For observation of surface morphology of fly ash particles, SEM images of unmilled and 30 min milled fly ash particles were taken. Figure 4 (b) and Figure 4 (c) showed that the milling destroyed a large proportion of the spherical morphology of unmilled fly ash and subsequently resulted into nano/micro fly ash with more active surfaces [36].

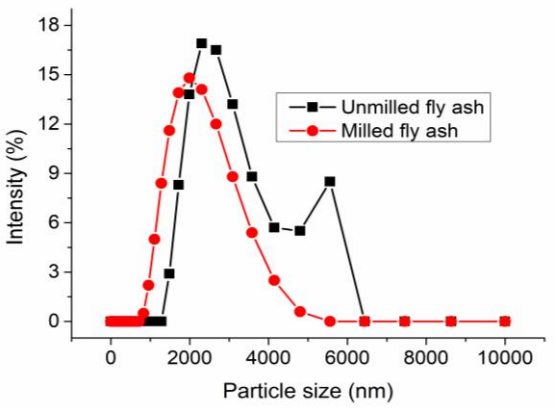

(a) Particle size distribution of fly ash

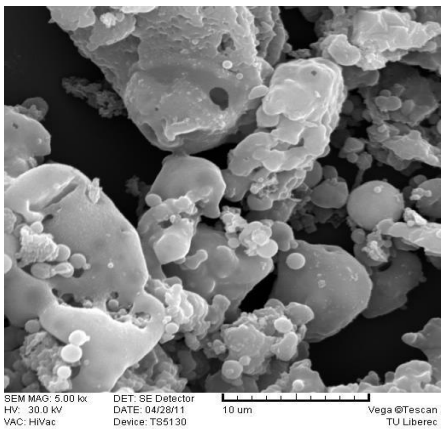

(b) SEM image of unmilled fly ash

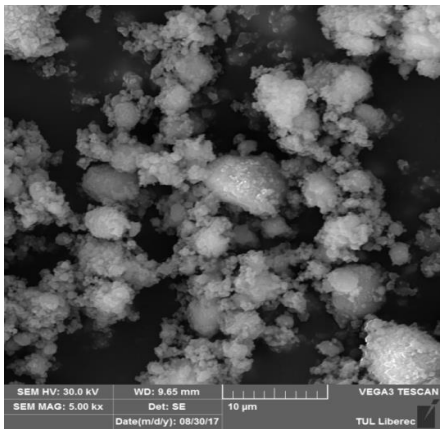

(c) SEM image of milled fly ash

Figure 4. Effect of ball milling on fly ash

5.1.2. Surface morphology of fly ash coated cotton fabrics

The surface hierarchical structure is important to obtain the superhydrophobic property. Figure 5 show the SEM images of fly ash coated fabric surfaces. The surface of cotton fiber was uniformly covered by fly ash particles. Moreover, dense coatings with obvious hierarchical structures were formed when increasing the fly ash concentration. A micro/nanoscale surface mimicking the surface of lotus leaf was formed with each fiber of approximately 10 μm diameter, and the fly ash particles of below 1000 nm size. A good adhesion between the fly ash particles and cotton fibers can be attributed to the presence of hydroxyl groups and formation of hydrogen bonds between them. Nevertheless, large particles observed on the textile surface with increase of fly ash concentration indicated their agglomeration tendency at high fly ash concentration [30].

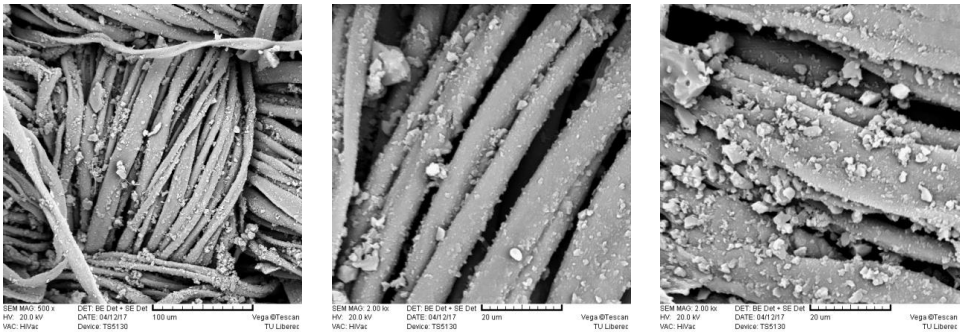

(a) 1 wt% fly ash (b) 2 wt% fly ash (c) 3 wt% fly ash

Figure 5. Surface structure of fly ash coated cotton fabrics

5.1.3. AFM analysis of fly ash coated cotton fabrics

The generation of surface roughness due to fly ash coating was further estimated using AFM. The AFM images and surface profiles of pristine and fly ash coated cotton fabrics are shown in Figure 6. For the pristine cotton fabric, the average roughness (Ra) was 22.56 ± 11.5 nm, and for fly ash coated cotton fabric, it was increased to 182.9 ± 15.7 nm, respectively. The pristine cotton fabric surface showed relatively smooth surface. It can be seen that after coating, the surface roughness of the fabric increased manifold. According to the Cassie-Baxter model, increasing surface roughness would increase the water contact angle of the surface [37]–[39].

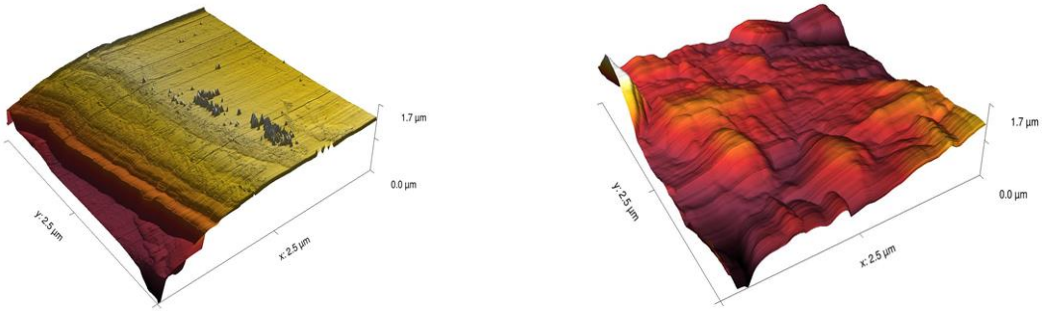

(a). Pristine cotton fabric (b). FA coated cotton fabric

Figure 6. AFM images of the pristine and coated fabrics

5.1.4. UV protection performance of fly ash coated cotton fabrics

Table 1 provides the average transmittance values of UV-A (315–400 nm), UV-B (280–315 nm) and the whole UV range (280–400 nm). The UV transmittance was found to reduce with increase in concentration of fly ash particles on fabric surface. The maximum UV blocking was observed in case of cotton fabric coated with 3 wt% fly ash, where the average transmittance decreased from 15.64%, 9.28% and 14.19% of the untreated fabric to 0.12%, 0.07% and 0.11% for UV-A region, UV-B region and the whole UV range, respectively. This behavior can be attributed to the absorbance of UV light by fly ash particles for transferring the electron from the valance band to the conduction band [40].

Table 1. UV transmission of fly ash coated cotton fabrics

Sample	UV-A (%)	UV-B (%)	Whole UV (%)	UPF
Without FA	15.64	9.28	14.19	9.49
1% MFA	0.56	0.33	0.50	299.4
2% MFA	0.23	0.14	0.21	801.44
3% MFA	0.12	0.07	0.11	1777.43

The ultraviolet protection factor (UPF) is another important parameter to assess the UV-blocking property of a fabric, which indicates the ability of fabrics to protect the skin against sun burning. It is defined as the ratio of potential erythemal effect to actual erythemal effect by the radiation transmitted through the fabric [41]. From Table 1, the untreated cotton fabric showed a low UPF of 9.49, however all the cotton fabrics decorated with fly ash particles exhibited large increase in UPF values. The maximum increase in UPF was observed for 3 wt% fly ash concentration, where the UPF value was increased to 1777.43. The great scattering of UV rays can be attributed to large refractive index of fly ash particles accompanied with constituents of metal oxides in their chemical composition [42].

5.1.5. Physical properties of fly ash-OTMS coated cotton fabrics

The add-on of coated fabrics at different fly ash-OTMS coatings were calculated, and it was found to increase in linear pattern with increase in fly ash concentration. The final dry add-on of the coated fabrics was measured as 2.5% for 1% FA+OTMS, 6.3% for 2% FA+OTMS and 9.2% for 3% FA+OTMS. Subsequently, the hand (i.e. comfort) properties of the coated fabrics were assessed from the measurements of stiffness values. Stiffness is a tendency of the fabric to keep standing without support. It is a special property of the fabric for desirable draping and also influences the physical comfort of clothing [43]–[45]. It can be evaluated from bending properties of the fabric using bending length and flexural rigidity. Despite large increments in add-on of coated fabrics at higher fly ash concentration, the stiffness values were found to increase marginally. The stiffness of uncoated cotton fabric was 0.86 N m, whereas it was measured as 1.09, 1.23 and 1.31 N m for 1%, 2% and 3% FA+OTMS coated cotton fabrics respectively. This indicated no loss in draping behavior of fly ash-OTMS coated cotton fabrics and therefore satisfactory physical comfort behavior.

5.1.6. Superhydrophobic properties of fly ash-OTMS coated cotton fabrics

The effect of fly ash particles on surface wettability of fly ash-OTMS coated cotton fabrics was investigated from measurements of static water contact angle, roll-off angle and contact angle hysteresis (see Figure 7). The surface of uncoated cotton fabric was completely wetted by the water droplet without any contact angle, whereas the water droplet exhibited a spherical shape on the surface of fly ash-OTMS coated textile (see Figure 1). For OTMS coated cotton fabrics, the static water contact angle and roll off angle were measured around 130^o and 21^o respectively. This indicated the hydrophobic behavior of cotton fabrics with OTMS coating alone, however the water droplets were difficult to roll off on this surface showing the strong adhesion between the water droplet and the coating surface. When fly ash particles were applied on cotton fabric with subsequent treatment of OTMS, the contact angle was enhanced and roll off angle was further decreased. The static contact angle of 143^o, 147^o and 153^o and roll off angle of 13^o, 8^o and 5^o was measured for fly ash concentration of 1, 2 and 3 wt% respectively (see Figure 7a). These results demonstrated the improvement in water repellency from surface hydrophobicity to superhydrophobicity when cotton fabric was coated with 3 wt% fly ash and then OTMS. From Figure 5, the enhancement in water repellency can be attributed to the formation of unique two-tier structural surface combined with the microscaled cotton fibers (10 μm) and the nanoscaled fly ash particles (below 1 μm). Further, the contact angle hysteresis (i.e. difference between the advancing and receding contact angles) plays an important role in the sliding behavior of water droplets for self-cleaning effect [46]–[48]. Therefore, the advancing and receding angles of fly ash-OTMS coated cotton fabrics were measured to examine the influence of fly ash particles on the self-cleaning effect. From Figure 7(b), the contact angle hysteresis was found to reduce from 11° to 6° with increase of fly ash concentration from 1wt% to 3 wt%. This indicated the formation of discontinuous, unstable, and contorted air/solid/liquid contact line at higher concentration of fly ash particles. By depositing high density of fly ash particles, solid–liquid–air contact line can further become more discontinuous and a larger amount of air film can be trapped leading to superhydrophobicity. Based on previous studies, a liquid droplet on a superhydrophobic surface can fulfill either Wenzel state or Cassie–Baxter state, or both [49]. A liquid impregnates the rough surface to form a completely wetted contact with the surface in the Wenzel state, whereas the liquid does not completely fill up the rough surface and there are air pockets trapped at the solid–liquid interface in the Cassie–Baxter state [42]. Therefore, the superhydrophobicity of the fly ash-OTMS coated cotton fabrics can be believed in Cassie–Baxter state where spherical water drop cannot penetrate entire fabric surface due to large amount of air trapped in the structure [28]. For verification of Cassie–Baxter state, the fly ash-OTMS coated cotton fabric was immersed into water by an external force (see Figure 1). A silver mirror-like bright and reflective surface was observed, which was attributed to the plastron layer formed by the trapped air between the water and the superhydrophobic fabric [50].

The physical self-cleaning behavior of 3 wt% fly ash-OTMS coated cotton fabrics was examined due to their superhydrophobic nature and low roll off angles. The orange dye was used as contaminants to test the self-cleaning ability. From Figure 8, the water drop was found to roll over the surface of the superhydrophobic fabric maintaining a spherical shape and subsequently the dye particles were taken away, leaving a clean trace on the superhydrophobic fabric [51].

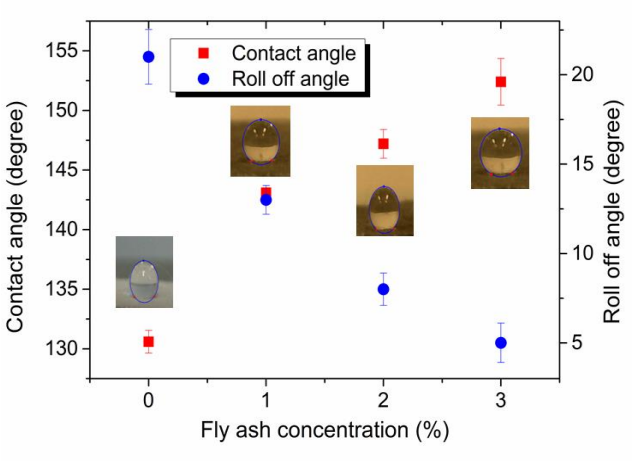

(a). Static contact angle

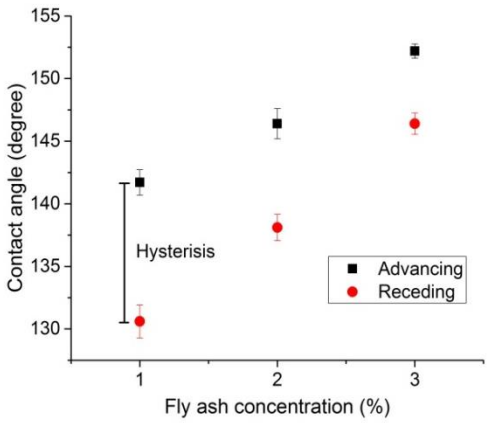

(b). Contact angle hysteresis

Figure 7. Effect of fly ash concentration on contact angle

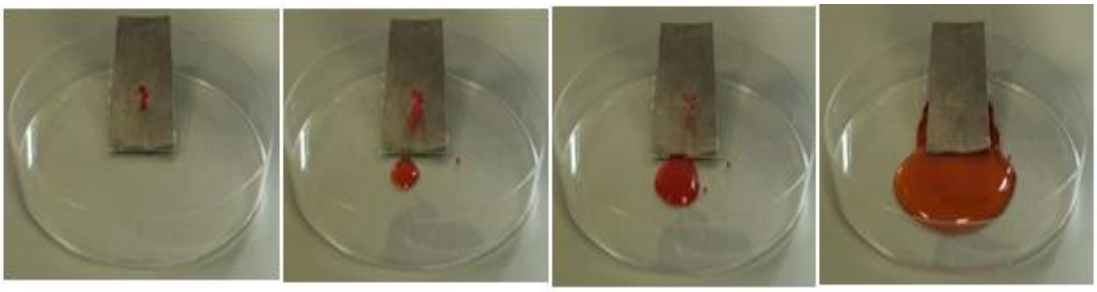

Figure 8. Self-cleaning property of 3 wt% fly ash-OTMS coated cotton fabric

5.1.7. Analysis of superhydrophobicity of fly ash-OTMS coated cotton fabrics

From Cassie–Baxter model, the area fraction of a water droplet (f) in contact with a fabric surface (i.e. wetted solid fraction) can be estimated based on the relationship between the apparent contact angle (θ^*) observed on a rough surface and the equilibrium contact angle (θ) obtained on a smooth surface. From Figure 9 (a), the wetted solid fraction was found to decrease with increase in surface density of fly ash particles. The increase in unwetted fraction of the air pocket trapped in the interspaces among the fly ash particles was estimated to be 43%, 55% and 67% respectively for 1, 2 and 3 wt% of fly ash particles. This confirmed that the layer of fly ash particles created a rougher surface for the air storage to resist liquid penetration.

Furthermore, the movement of liquid droplets on hydrophobic surfaces was described by calculation of work of adhesion (W_{ad}) according to the Young–Duprè equation [52] (see Equation 5).

$$W_{ad} = \gamma_L(1 + cos\theta) \quad (5)$$

Where γ_L is the surface tension of the liquid drops (i.e.72.8 mN/m).

Figure 9 (b) shows the inverse relationship between work of adhesion and the surface density of fly ash particles. The work of adhesion for OTMS coated cotton fabric was measured around 25.42 mN/m. On the other hand, values of work of adhesion for fly ash-OTMS coated cotton fabrics ranged from 14.58 to 8.28 mN/m. The fabric surface decorated with 3 wt% fly ash exhibited lowest

work of adhesion value, which indicated smallest work required for the movement of the water drop on its surface. Thus, an efficient way to improve the water repellency of cotton fabric was confirmed by creation of a fly ash layer with subsequent OTMS treatment. By equating the work of adhesion and the work of separation, the maximum force of attraction can be achieved [47]. By accepting the force versus distance relationship of attraction and repulsion, the attractive force ($\boldsymbol{F_a}$) and repulsive force ($\boldsymbol{F_r}$) at equilibrium can be written as given in Equation (6) and Equation (7), respectively.

$$F_a = (F_a)_e \left(\frac{d}{x}\right)^3 \tag{6}$$

$$F_r = (F_r)_e \left(\frac{d}{x}\right)^8 \tag{7}$$

Where x is the separation distance and d is the equilibrium distance

Under equilibrium conditions

$$(F_a)_e = (F_r)_e$$

Therefore, the work of adhesion can be expressed as given in Equation (8) and Equation (9) [52].

$$W_{ad} = \int_d^\infty (F_e)\left(\frac{d}{x}\right)^3 dx - \int_d^\infty (F_e)\left(\frac{d}{x}\right)^8 dx \tag{8}$$

Which is equal to

$$W_{ad} = F_e\left[\frac{d}{2} - \frac{d}{7}\right] \tag{9}$$

In this way, the force of attraction F_e can be determined by knowing the values of work of adhesion W_{ad} and equilibrium distance d. The distance between the molecular centers of a liquid can be estimated from the specific gravity and molecular weight of the liquids. For example, the equilibrium distance of 3.1 ˚A can be used for estimation of distance between the molecular centers of water. The interfacial tension of liquid and the natural characteristics of the substrate, such as surface geometry or porosity, polarity, and chemical composition, affect the absorption of solid–liquid interface [48].

The force of attraction was calculated from the values of work of adhesion based on Equation (8) and Equation (9). From Figure 9 (c), the force of attraction was found to decrease with increase in fly ash concentration. The force of attraction for OTMS coated cotton fabric was measured around 22.9 (10^{-8}dyne/cm^2). However, for cotton fabrics decorated with fly ash particles, the force of attraction ranged from 13.13 to 7.45 (10^{-8}dyne/cm^2). This suggested that it required only about half the force to move a water drop on the fabric decorated with 3 wt% fly ash compared to that with 1 wt% fly ash.

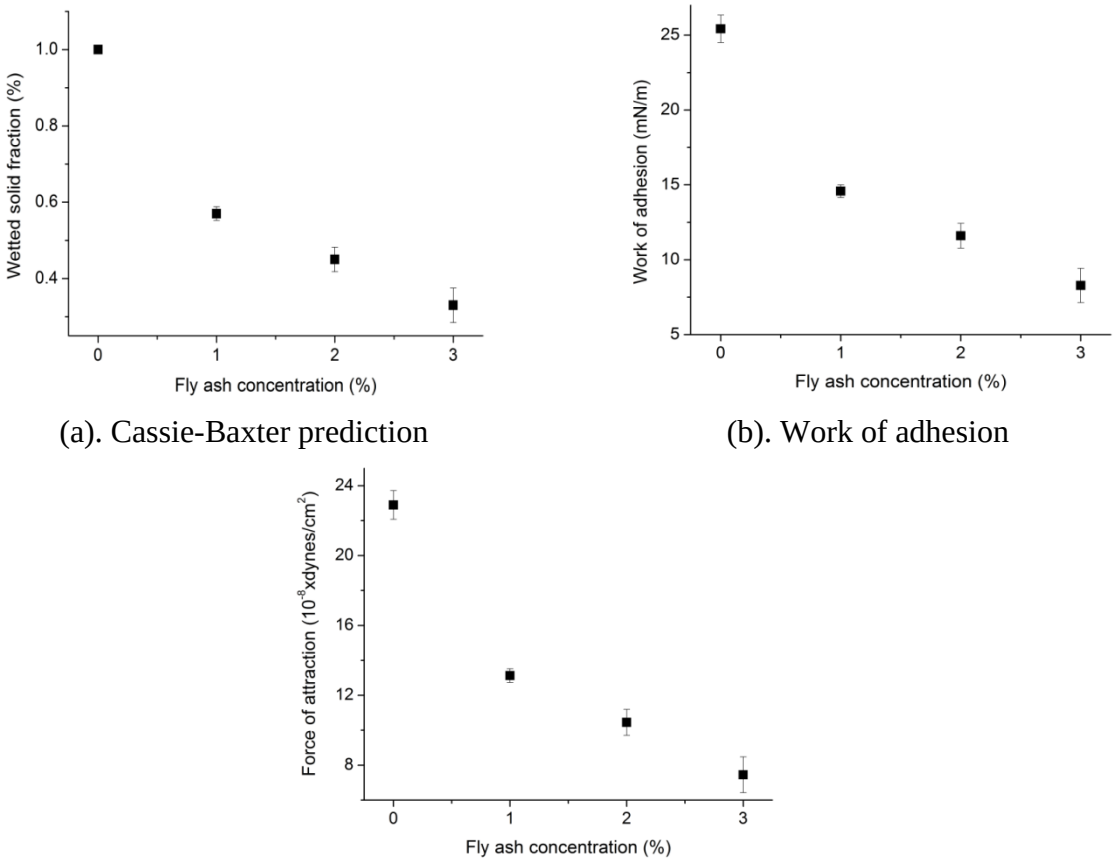

(a). Cassie-Baxter prediction (b). Work of adhesion

(c). Force of attraction

Figure 9. Analysis of superhydrophobicity of fly ash-OTMS coated cotton fabrics

5.1.8. Durability of superhydrophobic properties of fly ash-OTMS coated cotton fabrics

Figure 10 (a) shows the results of contact angle measurements for characterization of durability of fly ash-OTMS coated cotton fabrics against mechanical abrasion, laundering, chemical and UV action. It was observed that the water contact angles were reduced to some extent after 20 cycles of sand paper abrasion, but still maintained their superhydrophobicity especially at higher deposition of fly ash particles. Similarly, the contact angle was reduced for all the concentration of fly ash after five laundering cycles. However, it was still higher than 150^{o} for 3 wt% fly ash sample. This demonstrated that fly ash particles were robust and stable on cotton surfaces, and only few fly ash particles were removed due to shearing and friction forces of laundering process [6]. When chemical durability of superhydrophobic fly ash-OTMS coated cotton fabrics was studied, all samples showed significant reduction of contact angle against alkaline conditions (pH=13) whereas negligible reduction against acidic conditions (pH=1). In order to improve the durability of contact angle, one of the solutions is going from two-tier surface roughness to the three-tier surface roughness characteristics. The ultraviolet durability of superhydrophobic fly ash-OTMS coated cotton fabrics was studied as many types of materials lose their superhydrophobicity when exposed to ultraviolet irradiation [30]. The water contact angle had no obvious decrease for all the fly ash concentration, which indicated that fly ash coated samples have great resistance to ultraviolet rays and can be used under solar radiation. Finally, the durability of contact angle when fabric surface was impacted by jet of water can be observed from the time-lapse photographs of

water droplets bouncing on the fabric as shown in Figure 10 (b). The water droplets completely left the fabric surface without wetting, which further indicated the development of superhydrophobic fly ash-OTMS coated cotton fabrics.

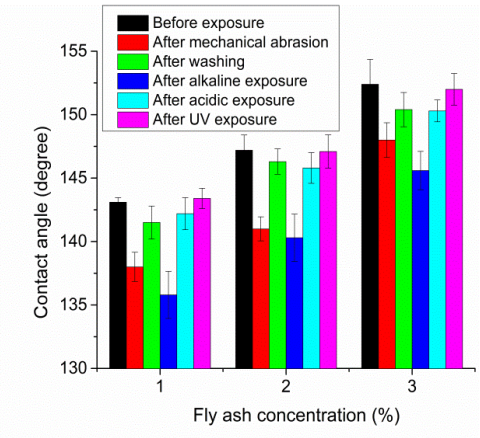

(a). Contact angle before and after exposure

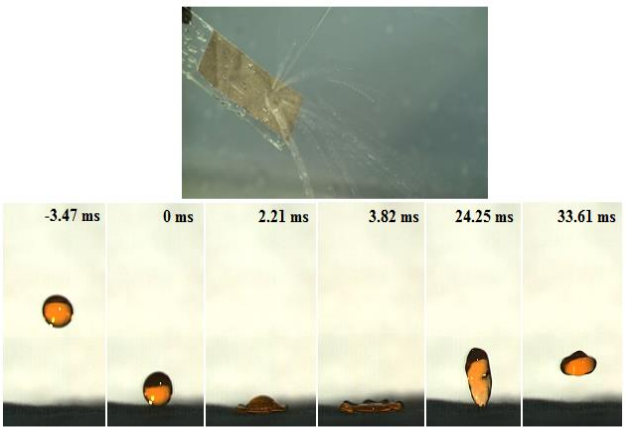

(b). Impact of water jet and bouncing of water droplets

Figure 10. Durability of fly ash-OTMS coated cotton fabrics

5.1.9. Oil in water removal performance of fly ash-OTMS coated cotton fabrics

As fly ash-OTMS coated cotton fabrics were superhydrophobic in nature, therefore further investigation was made on their oil sorption capacity. The toluene as model oil was used to observe the oil separation from the surface of water, whereas chloroform as model oil was used to observe the underwater oil separation performance. A small amount of toluene and chloroform oil dyed by red orange is added into the water surface. Due to low density of toluene, it was floated on water surface (Figure 11a). Whereas, chloroform reached to bottom of water surface due to its high density (see Figure 11b). When a piece of superhydrophobic fly ash-OTMS coated cotton fabric was immersed into the water, both the oils were completely absorbed into the coated fabric structure within few seconds without leaving any color in water. This improvement of oil retention ability can be attributed to enhanced stability of capillary pressure to prevent the sliding of absorbed oil on fiber surface by creation of rough surfaces by fly ash particles [53].

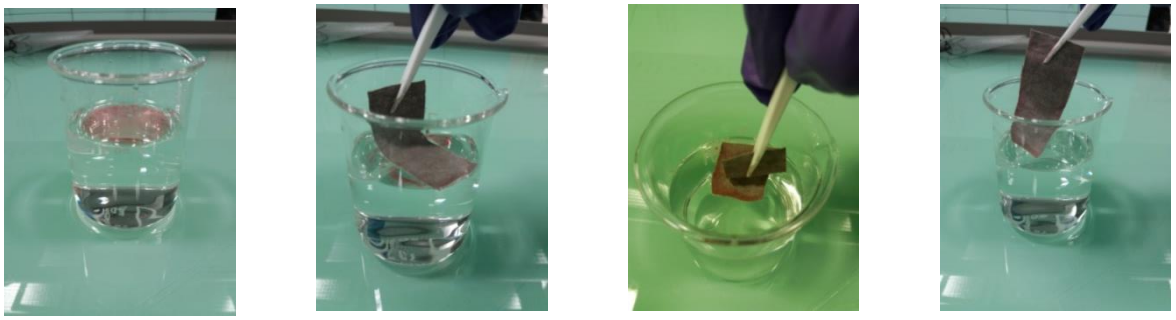

(a). Photographs of toluene removal from top water surface

(b). Photographs of chloroform removal from underwater surface

(c). Photographs of oil in water separation experiment

Figure 11. Oil in water removal performance of fly ash-OTMS coated cotton fabrics

Furthermore, the oil separation efficiency of fly ash-OTMS coated cotton fabrics was quantitatively estimated in separate experiments (see Figure 11c) using four model oils of different densities (i.e. toluene, n-hexane, chloroform and petro ether). When the mixture of oil (dyed with red orange) and water was poured onto the superhydrophobic textile, the oil was quickly passed through the coated fabric into the small beaker. On the other hand, water was accumulated on the cotton surface, and then decanted into the big beaker from the top of the coated fabric. The separation efficiency of 98%, 96%, 97% and 95% was obtained for toluene/water, n-hexane/water, chloroform/water and petro ether/water, respectively. Moreover, the oil absorption capacity for toluene, n-hexane, chloroform and petro ether was found around 2540, 1750, 3300, 2100 %, respectively. The difference in oil sorption capacity was mainly attributed to the viscosity, density and surface tension of oils [30]. Later, the oil absorption capacities of fly ash-OTMS coated cotton fabrics were compared with previously reported high performance oil-absorbents. For example, SiO_2/Octadecyltrichlorosilane coated cotton showed the oil absorption capacity of 4500 for chloroform [54], whereas polydimethylsiloxane coated cotton showed the oil absorption capacity of 2485 for toluene [55]. Although few studies showed better oil absorption capacities, however the results from the current study were found encouraging owning to low cost, and good environmental friendliness of fly ash particles. Therefore, the findings of this work could be useful for versatile separation of oil/water mixtures under various conditions (e.g. floating oil layer, underwater oil droplet or oil/water mixtures). Towards the end, the reusability of superhydrophobic fly ash-OTMS coated cotton fabric was investigated by measuring the separation efficiency for toluene/water and chloroform/water after numerous of water–oil

separation recycles. The oil sorption capacities decreased slightly throughout the whole cycles and the separation efficiency of coated fabrics ranged from 98% to 94% for toluene and 97% to 94% for chloroform after 5 cycles. The small decrease of oil sorption capacity can be attributed to the residual oils inside the structure of coated fabrics [56].

5.2. Superhydrophobic fabrics coated with TiO_2 nanoflowers and OTMS

5.2.1. SEM analysis of polyester fabrics coated with TiO_2 nanoflowers

The polyester fiber surface has low surface free energy, low wettability and poor adhesion due to lack of polar groups (COOH and OH) on the main chains. In order to attach TiO_2 nanoseeds on polyester fabric surface, the caustic soda treatment was carried out to generate the polar groups. Although the tensile strength of the polyester fabric decreased by 11 % due to the cleavage of ester linkages and hydrolysis of polyester chains, but it resulted into the formation of hydroxyl and carboxyl acid groups on the fiber surface [57]. From Figure 12b, Oligomers formed due to hydrolysis of polymer chains can be seen as small particles on the surface of the polyester fibers. The attachment of very fine TiO_2 nanoseeds can be observed from the surface of polyester fibers shown in Figure 12c.

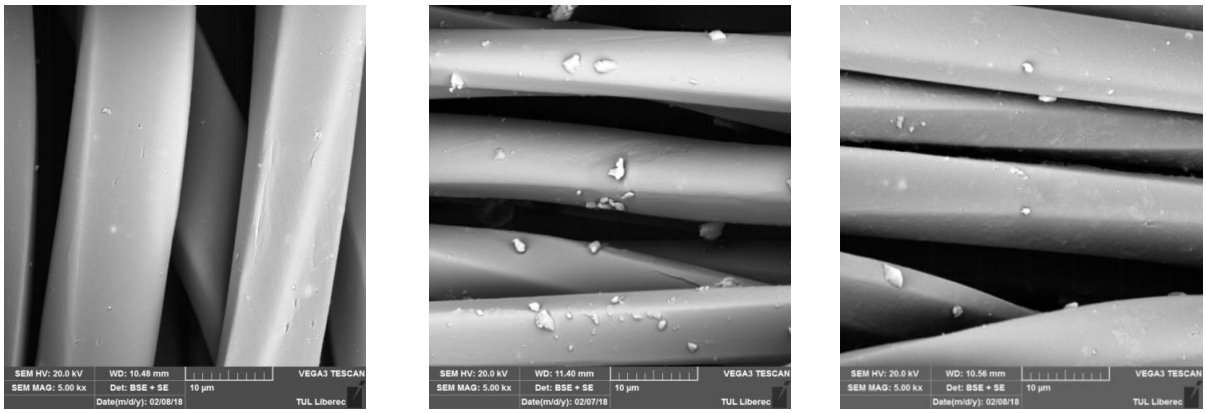

(a) Before caustic soda (b) After caustic soda (c) After seeding

Figure 12. SEM micrographs of polyester fabric

The surface hierarchical structure is important to obtain the superhydrophobic property. The surface structure of coated fabrics was investigated at different TTIP doses (i.e. 0.5 mL, 1 mL, 1.5 mL, and 2 mL) from SEM images shown in Figure 13. It can be seen that the dose of TTIP had a great effect on the growth and structure of TiO_2 nanoflowers. At low dose of TTIP (i.e. 0.5 mL), no TiO_2 flower structures were found on the polyester fiber surface except some tiny crystal nuclei of TiO_2 particles. However, the amount and the size of TiO_2 flower structures greatly increased as the amount of TTIP increased from 1 mL to 1.5 mL (see Figure 13a and Figure 13b). When the TTIP dose was further increased to 2 mL (see Figure 13c), the flower-like structures started to aggregate sharply and a continuous thicker coating was constructed on the polyester fiber surface. A micro/nanoscale surface mimicking the surface of lotus leaf was formed with each fiber of approximately 10 µm diameter, and the TiO_2 particles of below 500 nm sizes. A good adhesion between the TiO_2 particles and polyester fibers can be attributed to the presence of hydroxyl groups and formation of hydrogen bonds between them.

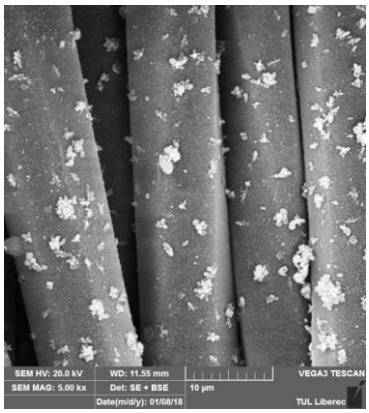

(a) 1 mL TTIP

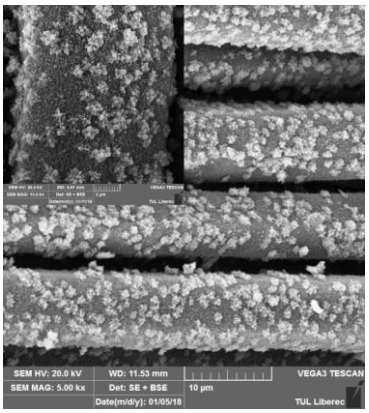

(b) 1.5 mL TTIP

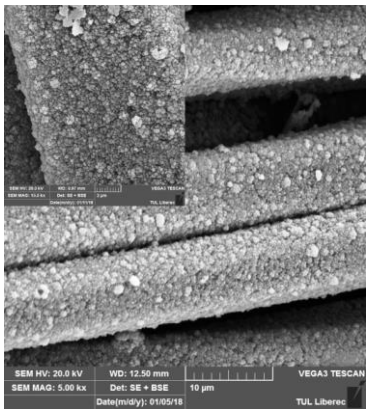

(c) 2 mL TTIP

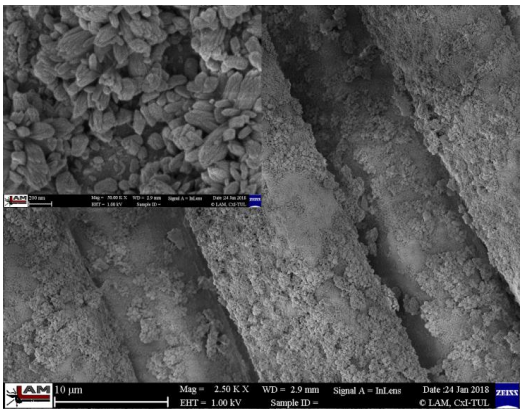

(d) 2mL TTIP with high resolution

Figure 13. Effect of Titanium isopropoxide dose on growth of TiO_2 nanoflowers

5.2.2. EDS analysis

It was carried out to know the chemical composition of TiO_2 coated fabric. The EDS spectra in Figure 14 showed the presence of O, C, Ti, and Au as main elements on the surface of TiO_2 coated fabric, whereas the pristine polyester surface mostly consisted of O and C elements. The relative atom ratio for O, C, and Ti was determined about 40.7%, 37.1%, and 22.1%, respectively. The presence of Au element was caused by sputtering of gold on TiO_2 coated sample during SEM characterization.

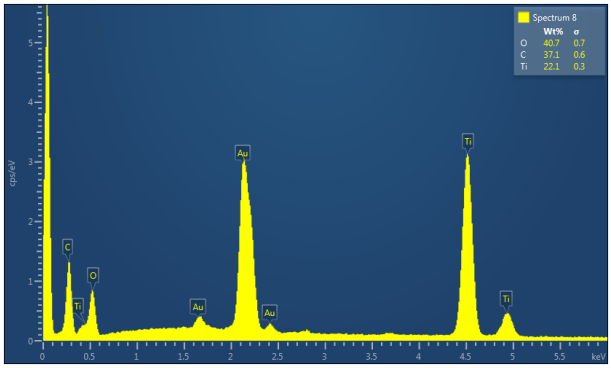

Figure 14. EDS spectrum of flower-like TiO_2 nanoparticles coated on polyester

5.2.3. Raman spectroscopy

It was employed to investigate the crystal structure of TiO_2 flower shaped 3D structures coated on the polyester fabrics. The Raman spectra shown in Figure 15 displayed the vibration modes at about 231, 447, and 608 cm^{-1}, which can be attributed to the second-order Raman scattering of tetragonal structure. The Raman peak observed at 146 cm^{-1} indicated the formation of the anatase TiO_2 phase [58], [59], whereas the two strong Raman peaks observed at 447 cm^{-1} and 608 cm^{-1} confirmed the formation of crystalline rutile phase [60]–[62]. The intensity and peak positions of observed Raman spectra are in good agreement with the previous studies reported in the literature.

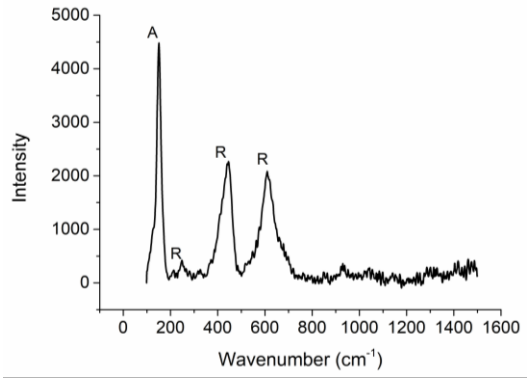

Figure 15. Raman spectra of flower-like TiO_2 nanoparticles coated on polyester fabric

5.2.4. XRD analysis

It was carried out to determine the crystal phase of the complex TiO_2 nanostructures coated onto polyester fabrics. As discussed in previous section of Raman spectroscopy, the existence of both anatase and rutile TiO_2 phases in the synthesized TiO_2 flower structures were confirmed (see Figure 16) [61]. The Bragg peaks observed at 27.08, 36.02, 41.24, 54.26 and 62.89 (2θ) were due to (110), (101), (111), (211) and (002) planes of tetragonal rutile phase (JCPDS no. 76-0317). The peaks observed at 25.29 and 48.01 (2θ) were due to (101) and (200) planes of the anatase phase (JCPDS no 21-1272) [63], [64]. Further, the shapes of the diffraction peaks suggested the formation of highly crystalline TiO_2 structures. It was found that the ratio *R* of the intensity of the strongest rutile reflection I_r to the intensity of the strongest anatase reflection I_a (i.e. $R = \frac{I_r}{I_a}$) on XRD pattern can be used for quantification of TiO_2 individual polymorphs content. The weight fraction of anatase x_a can be approximated by Equation (10) [65].

$$x_a = \frac{1}{1.265\,R + 1} \tag{10}$$

From the XRD pattern the ratio *R* was estimated around 0.698 and by using above Equation the weight fraction of anatase x_a of flower-like TiO_2 nanoparticles coated on polyester fabric was calculated 0.532.

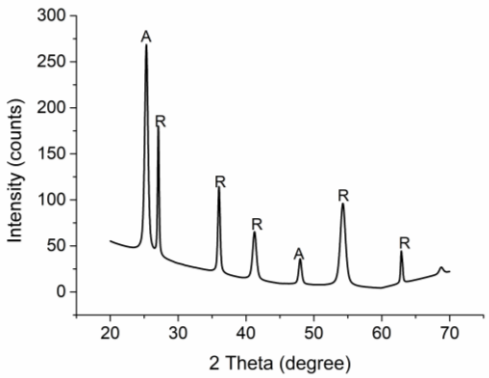

Figure 16. XRD pattern of flower-like TiO_2 nanoparticles coated on polyester fabric

5.2.5. AFM analysis

Figure 17 shows the topographical AFM images and surface profiles of the TiO_2 coated polyester fabrics. The increase in surface roughness of the coated polyester fabric can be seen from the topographical image. The average roughness (Ra) of 78.8 ± 9.3 nm was estimated for the flower-like TiO_2 nanoparticles coated polyester. Such surface roughness is sufficient to fabricate the physical self-cleaning (lotus effect) combined with hydrophobic surface chemistry by OTMS coating. The micro/nano structures enhance the roughness, which is necessary to form air cushion and validation of the Cassie–Baxter equation.

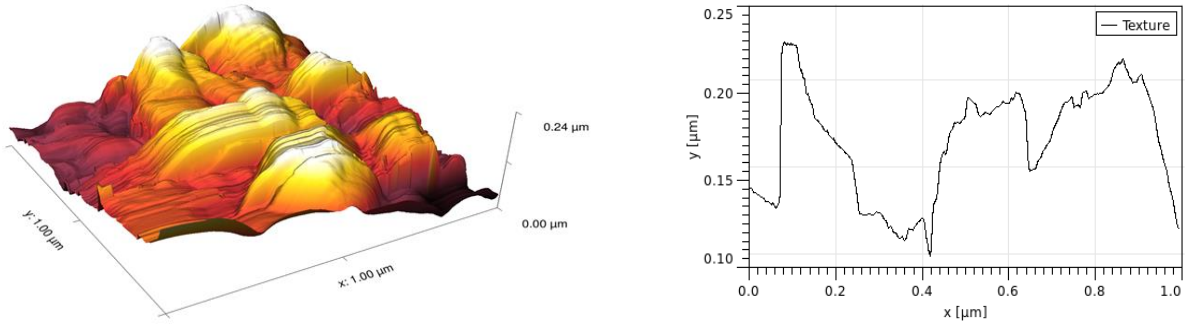

(a). 3D AFM image (b). Surface profile

Figure 17. AFM analysis of the flower-like TiO_2 nanoparticles coated polyester

5.2.6. Physical properties of TiO_2-OTMS coated polyester fabrics

The add-on of coated fabrics at different TiO_2-OTMS coatings were calculated, and it was found to increase in linear pattern with increase in TTIP dose. The final dry add-on of the coated fabrics was measured as 1.8 % for 1 mL TTIP, 4.2 % for 1.5 mL TTIP and 7.3 % for 2 mL TTIP doses. Despite large increments in add-on of coated fabrics at higher TTIP dose, the stiffness values were found to increase marginally. The stiffness of uncoated polyester fabric was 0.93 N m, whereas it was measured as 1.16, 1.32 and 1.42 N m for TiO_2+OTMS coated polyester fabrics at 1 mL, 1.5 mL and 2 mL TTIP respectively. This indicated no loss in draping behavior of TiO_2-OTMS coated polyester fabrics and therefore satisfactory physical comfort behavior.

5.2.7. Superhydrophobic properties of TiO_2 nanoflowers coated polyester fabrics

The measurements of static water contact angle, roll-off angle and contact angle hysteresis were made to understand the effect of surface decoration of TiO_2 flowers on surface wettability of TiO_2-OTMS coated polyester fabrics (Figure 18). Without any decoration of TiO_2 flowers and with only coating of OTMS on polyester surface, the static water contact angle and roll off angle were measured around 129.8º and 15º respectively. When polyester fabric surface was decorated with 3D shaped TiO_2 flowers and subsequent treatment of OTMS, the enhancement in contact angle and simultaneous reduction in roll off angle was found. The increase in contact angle and reduction in roll of angle was observed with the increase of TTIP dose during the hydrothermal deposition of TiO_2 flowers (Figure 18a). The maximum static contact angle of 160.1º and minimum roll off angle of 3º was found for 2 mL TTIP dose. Therefore, the improvement in water repellency from surface hydrophobicity to superhydrophobicity can be confirmed when polyester fabric surface is decorated with TiO_2 nanoflowers before the OTMS coating. This phenomenon can be attributed to the formation of unique two-tier structural surface combined with the microscaled polyester fibers (10 μm) and the nanoscaled TiO_2 flowers (500 nm).

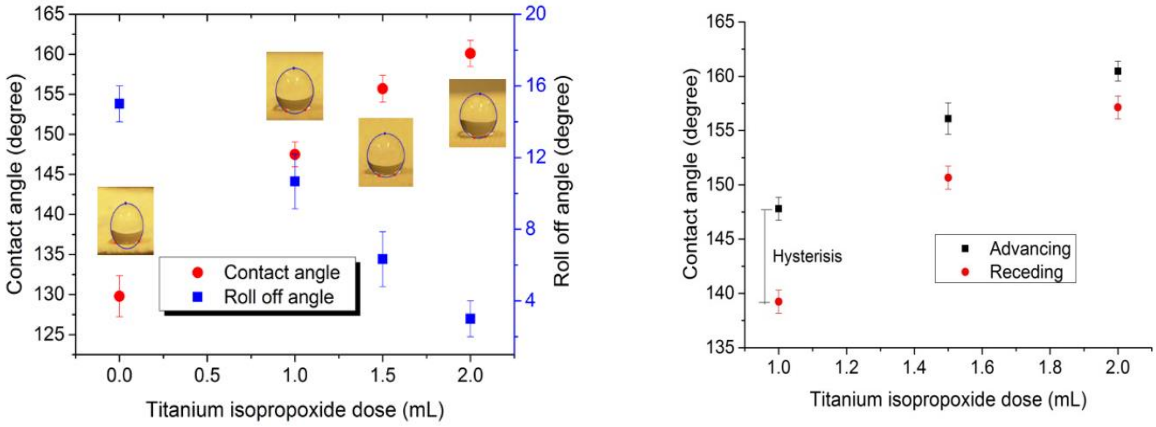

(a) Static contact angle (b) Contact angle hysteresis

Figure 18. Effect of Titanium isopropoxide dose on contact angle

The contact angle hysteresis (i.e. difference between the advancing and receding contact angles) plays an important role in the sliding behavior of water droplets for self-cleaning effect [46], [47]. Here, the advancing and receding angles of TiO_2-OTMS coated polyester fabrics were measured to examine the influence of TiO_2 flower structures on the self-cleaning effect. From Figure 18b, the contact angle hysteresis was found to reduce from 9° to 3° with increase of TTIP dose from 1 mL to 2 mL, which indicated the formation of discontinuous, unstable, and contorted air/solid/liquid contact line due to the decoration of TiO_2 flowers. For superhydrophobicity, the solid–liquid–air contact line can further become more discontinuous and a larger amount of air film can be trapped by depositing high density of TiO_2 flowers using higher dose of TTIP.

5.2.8. Analysis of superhydrophobicity of coated polyester fabrics

The Cassie–Baxter model can be used to estimate the area fraction of a water droplet (f) in contact with a fabric surface (i.e. wetted solid fraction) from the relationship between the apparent contact angle (θ^*) observed on a rough surface and the equilibrium contact angle (θ) obtained on a smooth surface. It can be seen from Figure 19(a) that the wetted solid fraction was decreased with increase in surface density of TiO_2 nanoflowers. The increase of 58%, 78% and 83% unwetted fraction of

the air pocket was observed for the dose of 1 mL, 1.5 mL and 2 mL TTIP respectively, which further confirmed that the layer of TiO_2 nanoflowers created a rougher surface for the air storage to resist liquid penetration. Furthermore, the Young–Duprè equation was employed to describe the movement of liquid droplets on hydrophobic surfaces by calculation of work of adhesion (W_{ad}). The work of adhesion was found to reduce with increase in surface density of TiO_2 nanoflowers (see Figure 19b). The polyester fabric coated with OTMS alone depicted the work of adhesion around 26.2 mN/m, whereas it ranged from 11.4 to 4.34 mN/m for TiO_2-OTMS coated polyester fabrics at respective doses of TTIP from 1 to 2 mL. The least work of adhesion (or smallest work required for the movement of the water drop) was shown by fabric surface after decoration of TiO_2 nanoflowers at 2 mL TTIP dose.

At the end, the force of attraction F_e was estimated by knowing the values of work of adhesion W_{ad} and equilibrium distance d given. The force of attraction was found to decrease with increased deposition of TiO_2 nanoflowers on the surface (Figure 19c). The force of attraction for polyester fabric coated with OTMS alone was measured around 23.6 (10^{-8}dyne/cm^2). But, the force of attraction ranged from 10.27 to 3.9 (10^{-8}dyne/cm^2) after the decoration of TiO_2 flower structures at TTIP doses of 1 to 2 mL. This indicated less force required for movements of water drops on the fabric surface coated with increased amount of TiO_2 flowers and OTMS.

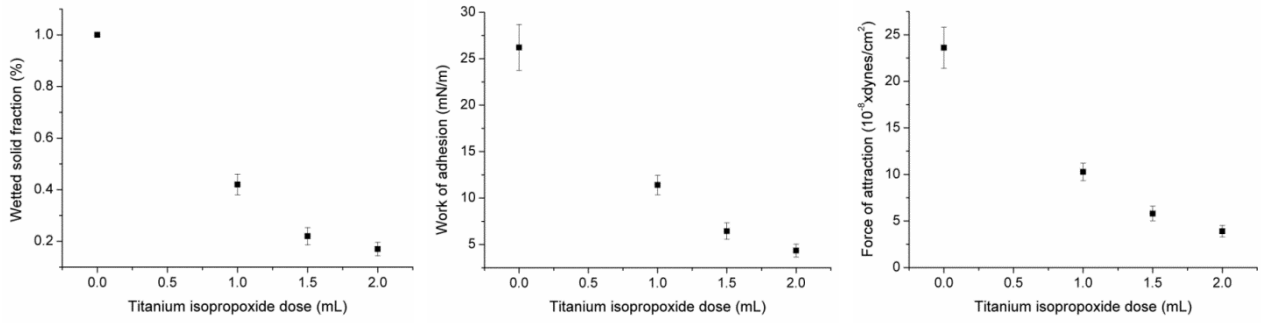

(a). Cassie-Baxter prediction (b). Work of adhesion (c). Force of attraction

Figure 19. Analysis of superhydrophobicity of TiO_2-OTMS coated polyester fabrics

5.2.9. Durability of superhydrophobic properties of coated polyester fabrics

The durability of TiO_2-OTMS coated polyester fabrics against mechanical abrasion, laundering, chemical and UV action can be seen from the results of contact angle measurements shown in Figure 20(a). After 20 cycles of sand paper abrasion, the water contact angles were reduced for all the samples of different TiO_2 depositions. However, the samples coated with TTIP doses of 1.5 and 2 mL continued to maintain their superhydrophobicity and presented the respective contact angles of 153^o and 156^o after mechanical abrasions. Likewise, the action of five laundering cycles resulted in the decrease of contact angles, but still higher than 150^o for the samples coated with more than 1.5 mL TTIP. The removal of only few particles for samples coated with TTIP dose of 1.5 and 2 mL against laundering indicated the robust and stable coating of TiO_2 particles over polyester fabrics [6]. Further, all samples showed acceptable reductions in superhydrophobic properties after exposure to chemical environment. The reductions in contact angle after exposure to alkaline environment was found greater than the acidic environments due to the itching of polyester fiber surfaces in presence of alkali. As many types of materials lose their superhydrophobicity when exposed to ultraviolet irradiation, therefore the ultraviolet durability of superhydrophobic TiO_2-OTMS coated polyester fabrics was also studied [30]. Compared to

mechanical and chemical actions, the water contact angle of coated fabrics was not affected after exposure to ultraviolet rays and thus suitable for use under the solar radiations (Figure 20a). Lastly, the effect of jet of water when impacted on coated fabric surface was examined to verify the durability of contact angles. The time-lapse photographs of water droplets bouncing on the fabric are shown in Figure 20(b), where water droplets completely left the fabric surface without wetting and thus confirmed their super hydrophobic behavior.

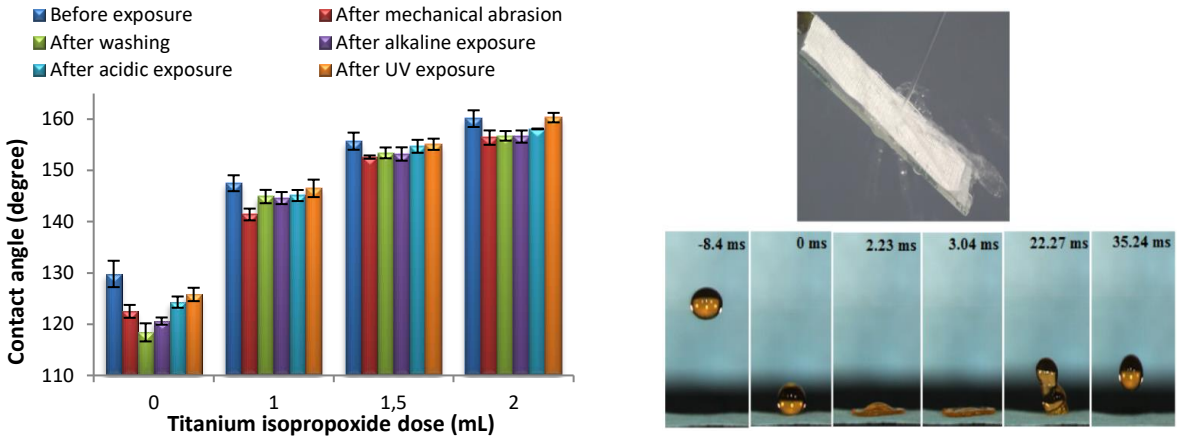

(a). Contact angle before and after exposure

(b). Impact of water jet and bouncing of water droplets

Figure 20. Durability of TiO_2-OTMS coated polyester fabrics

5.2.10. Physical self-cleaning properties of coated fabrics

Due to the superhydrophobic behavior and low roll off angles, the utility of TiO_2-OTMS coated polyester fabrics was studied for physical self-cleaning performance. The methyl orange dye was used as contaminant to demonstrate the self-cleaning action. When the water droplets were dropped on the contaminated fabric, it rolled over the surface and maintained the spherical shape. During the sliding process of water droplets, the dye particles were immediately picked up and taken away leaving behind a clear surface as seen in Figure 21 [51]. This behavior was attributed to the creation of lotus effect by high water surface tension and low surface energy of coated fabrics [66].

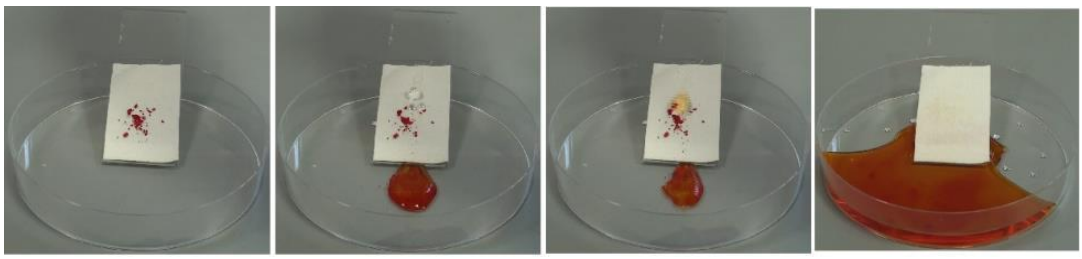

Figure 21. Physical self-cleaning property of TiO_2-OTMS coated polyester fabric

5.2.11. Chemical self-cleaning properties of coated fabrics

The chemical self-cleaning properties of coated fabrics were examined based on two aspects (i.e. stain degradation and solution discoloration tests). For stain degradation performance, the methyl orange dye was applied as stain on the coated fabrics and their photo degradation behavior towards

the dye was observed at different time intervals of exposure to the ultraviolet light. From Figure 22, the significant degradation of methyl orange dye was found for all the coated samples decorated with different concentrations of 3D shaped TiO_2 flowers. The reasons for low deviation under 30 min could be due to different locations of dyes and photocatalyst. When the dye stain was deposited on the coated fabric, the part of it which was on top of the TiO_2 nanoflowers degraded quickly because it was completely exposed to UV light. On the other hand, the dye deposited on the sides of nanoflowers required more time to degrade. The stains disappeared mostly within 3 h and the samples became approximately white after 4 h. Furthermore, the degradation rate was found to increase with increased density of TiO_2 flowers coated onto fabric and also with increased time of UV exposure. On the other hand, the pristine polyester fabrics showed no change in stain reduction even after the exposure to UV light for more than 4 h.

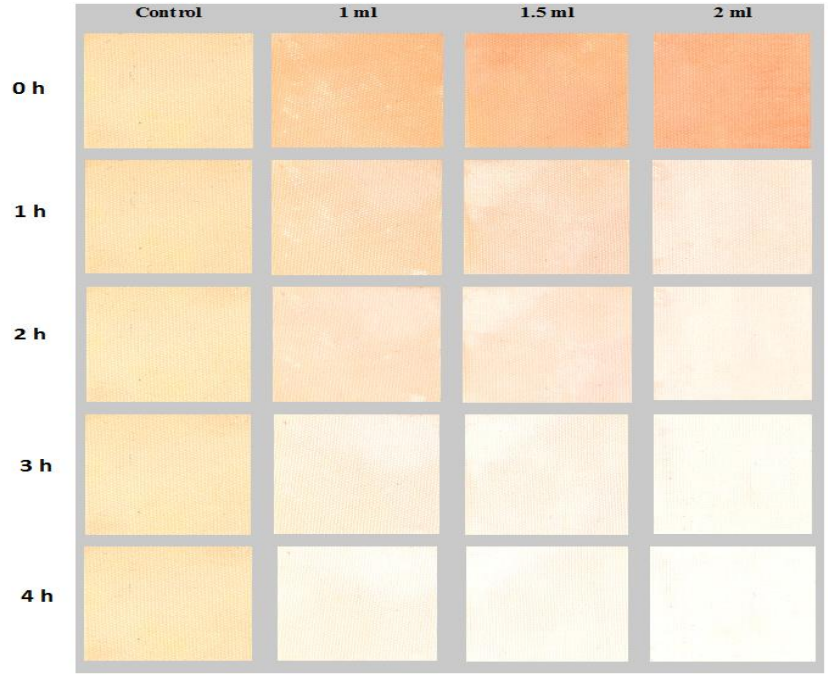

Figure 22. Photocatalytic stain degradation of TiO_2-OTMS coated polyester fabric

Later, the photocatalytic degradation rate of methyl orange dye was quantitatively estimated by measuring the color intensity of samples on ImageJ software. When the sample becomes whiter, the value (counts) of color intensity increases that mean it is measuring the whiteness of the sample. The increase in measured color intensity from this software can be correlated to increase in the whiteness index (see Figure 23). Interestingly, the depth of stains were found much higher before the start of UV irradiation on samples decorated with TiO_2 flowers than the alone OTMS coated sample. This can be attributed to hydrophilic nature of TiO_2 particles deposited onto the polyester fabrics. However, from the measurements of color intensity, the dye degradation of samples decorated with TiO_2 flowers was found to increase after the UV irradiation. Whereas, the sample coated with OTMS alone showed a straight line and thus no degradation of dyes in absence of TiO_2 particles. The photocatalytic activity of TiO_2 coated textiles can be attributed to the decomposition of dyes by generation of highly oxidative radicals under the UV light [11].

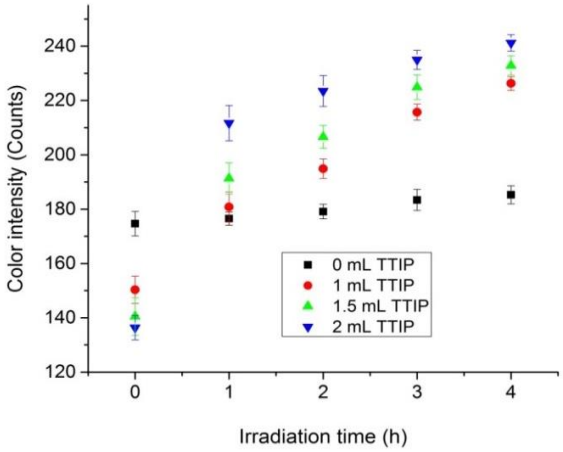

Figure 23. Evaluation of TiO_2-OTMS coated polyester fabric after photocatalytic degradation

Another test of solution discoloration was also employed to characterize the chemical self-cleaning properties of coated fabrics. Here, the coated samples were added into the dye solution and then the dye concentration was measured by recording the UV-Vis spectra. Figure 24(a) showed the absorbance spectra of the dye solution at different UV illumination time. The straight line obtained for the pristine polyester fabric indicated the absence of any photocatalytic activity by polyester itself. The absorbance value of methyl orange dye in the solution was measured by observing the peak intensity at 485 nm. The decrease in absorbance value with the passage of time indicated the decrease in the concentration of dye due to its photocatalytic degradation. The samples coated with 2 mL TTIP decolorized the dye solution in 150 min, whereas the samples coated with 1 mL and 1.5 mL TTIP took almost 300 and 210 min respectively. The higher rate of dye degradation in case of 2 mL of TTIP can be attributed to the decoration of high density 3D shaped TiO_2 flowers on the fiber surface. Furthermore, the photocatalytic efficiency of the sample coated with 2 mL TTIP was examined for repeated discolorations of dye solution. From Figure 24(b), no change in photocatalytic efficiency of treated fabric was found during the five successive discoloration cycles which confirmed its potential use for several times in the application.

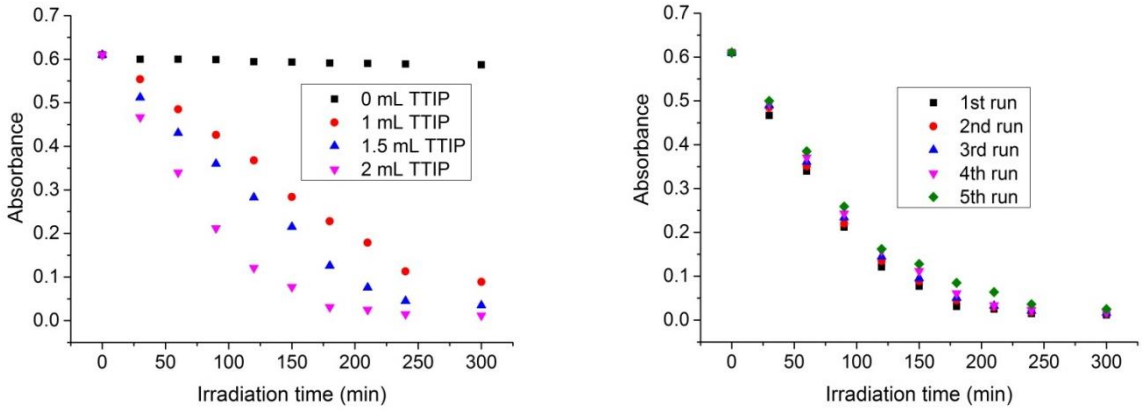

(a) Effect of TTIP dose (b) Effect of successive reuse cycles

Figure 24. Solution discoloration properties of TiO_2-OTMS coated polyester fabrics

5.3. Superhydrophobic fabrics coated with ZnO nanorods and OTMS

5.3.1. Morphological analysis and growth mechanism

The low surface energy and hierarchical micro/nanostructures are important factors to fabricate superhydrophobic textile surfaces. Microwave hydrothermal method was used for rapid growth of ZnO nanorods on the fiber surfaces to develop micro/nanostructures and then subsequently treated with low surface energy material (OTMS) to produce superhydrophobic surface. The surface of the pristine cotton fabric was completely wetted by the water droplet without any contact angle (inset, Figure 25a). From SEM image uniform and continuous layer of nanorods can be seen on the surface of the cotton fiber (Figure 25b), whereas; the water droplet exhibited a spherical shape on the surface of OTMS modified ZnO nanorods decorated cotton fabric (inset, Figure 25b). AFM image show topography of the grown ZnO nanorods on fibers of the cotton fabrics (Figure 25c). These results show the uniform patterned growth of the nanorods on the surface of the cotton fabrics. The grown nanorods enhance the surface roughness, which is necessary to form air pockets.

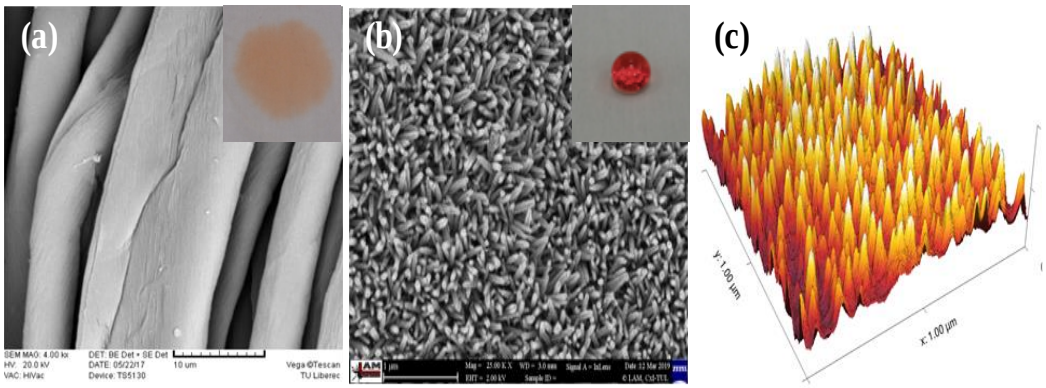

Figure 25. SEM image of the (a) pristine cotton fabric, (b) ZnO nanorods grown fabric surface and (c) 3D AFM image of the ZnO nanorods decorated fabric surface. Insets (a) and (b) are images of water droplet on the corresponding fabric surfaces.

The reaction taking place in the presence of $Zn(NO_3)_2 \cdot 6H_2O$ and HMTA during the growth of ZnO nanorods onto cotton fiber are given in equations (11) – (16).

$$C_6H_{12}N_4 + 6H_2O \rightarrow 6H_2CO + 4NH_3 \quad (11)$$

$$NH_3 + H_2O \rightarrow NH_4^+ + OH^- \quad (12)$$

$$Zn(NO_3)_2 \rightarrow Zn^{2+} + 2NO_3^- \quad (13)$$

$$Zn^{2+} + 2HO^- \rightarrow Zn(OH)_2 \quad (14)$$

$$Zn(OH)_2 \rightarrow ZnO + H_2O \quad (15)$$

$$Zn^{2+} + 4NH_3 \rightarrow [Zn(NH_3)_4]^{2+} \quad (16)$$

The hydrolysis of HMTA in aqueous solutions generates NH_4^+ and OH^- ions as shown in the Equation (12). The Zn^{2+} and $2NO_3^-$ ions released from hydrolysis of $Zn(NO_3)_2$ as shown in

Equation (13). The reaction of Zn^{2+} ions with OH^- ions to produce $Zn(OH)_2$ is given in eqn. (14). When $Zn(OH)_2$ is heated to 100 °C ZnO nanorods is formed as given in Equation (15). Moreover, the rest of Zn^{2+} ions and the ammonia formed in previous eqn. (11) react to form the $[Zn(NH_3)_4]^{2+}$ complex ions, as given in Equation (16).

The nanoseeds prior to growth of nanorods actually provide the site for nucleation which is prerequisite for growth of nanorods. Another important thing which favors the seeded growth is the presence of -OH groups on seeds which are similar to those present on (0001) face of ZnO crystals. The ZnO crystal in hexagonal wurtzite type structure has polar and nonpolar planes. The top polar (0001) plane is positively charged and exhibits high surface energy. The ZnO crystal growth under hydrothermal condition has fastest rate in this direction (0001). The shape and orientation of the grown ZnO nanocrystals are mainly influenced by the type and concentration of the ZnO precursors, additives, and pretreatment of substrate and deposition parameters, such as microwave power and deposition time [67]–[69].

To investigate the influence of the zinc nitrate hexahydrate and HMTA concentration on the growth and morphology of ZnO nanorods, a set of experiments was performed. The attachment of very fine ZnO nanoseeds can be seen on the surface of cotton fibers as shown in Figure 26(a). It was found that concentration of zinc nitrate hexahydrate and HMTA had a great influence on the size and structure of grown nanorods. At a low zinc nitrate hexahydrate and HMTA concentration of 10mM (Figure 26b), no ZnO nanorods were found on the surface of cotton fiber but only few tiny ZnO crystals were sparsely coated on cotton fiber surface.

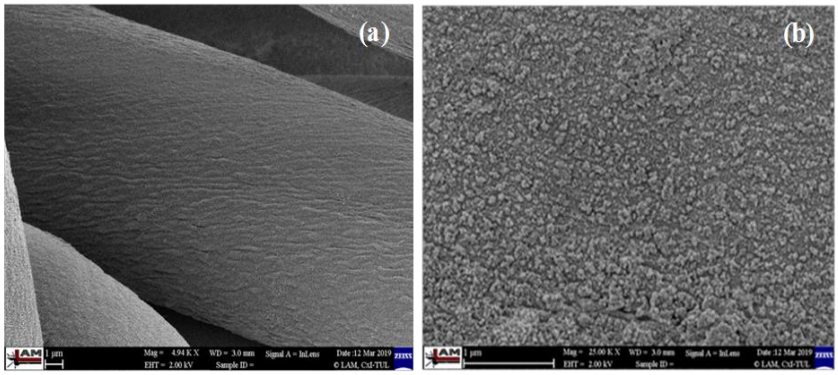

Figure 26. SEM images of (a) ZnO seeded cotton fiber and, (b) 10 mM zinc nitrate hexahydrate concentration treated cotton fiber

Figure 27 shows the SEM images of grown nanorods on cotton fiber surface at different level of concentrations (i.e., 25 mM to 100 mM). A uniform and continuous layer of grown ZnO nanorods can be seen on all the samples synthesized at different concentration. SEM images and Image J software was used for the calculation of the nanorods dimensions. An average value of the dimensions was calculated from 100 individual nanorods. The hexagon shaped morphology of the as-grown nanorods can be seen from SEM images. It is clear that the solution concentration plays a vital role in determining the shape and size of the ZnO nanostructures [70]. It was found that diameter (D) and length (L) of the as-grown nanorods increased with increased in concentration of zinc nitrate hexahydrate/HMTA (Table 2). The diameter and length of the as-prepared nanorods were found in the range of 35-55 nm (Diameter) and 190-300 nm (Length), respectively. The average diameter of the grown nanorods was increased from 35 nm to 55 nm, as the concentration

increased from 25 mM to 100 mM. The maximum length (300 nm) of the as-grown nanorods was achieved, when the 50 mM concentration of zinc nitrate hexahydrate/HMTA was used. When the ZnO rods were grown at higher concentration (i.e. 75 mM, 100 mM), more thick nanorods were obtained as compared to the lower concentration (i.e. 25 mM, 50 mM). These results shows that at higher concentration the growth increases more along the, $10\bar{1}0$ or $01\bar{1}0$ ZnO crystal planes that form the sides of ZnO hexagonal rods rather than the length direction (0001). Our results reveal that concentration plays an important role in the formation of the nanorods. Higher concentration led to the supersaturation and formation of many nuclei of small size which results in fast nucleation and slow growth rate. Thus, this will hinder the growth rate of the (0001) plane and making nanorods thicker [71]–[73].

Table 2. Dimension of nanorods grown at various concentrations

$Zn(NO_3)_2 \cdot 6H_2O$ Concentration (mM/L)	Nanorods average diameter (nm)	Nanorods Average length (nm)
25	35 ±3.5	190 ±11.5
50	41 ±5.4	300 ±14.6
75	50 ±4.2	262 ±12.6
100	55 ±6.1	260 ±15.4

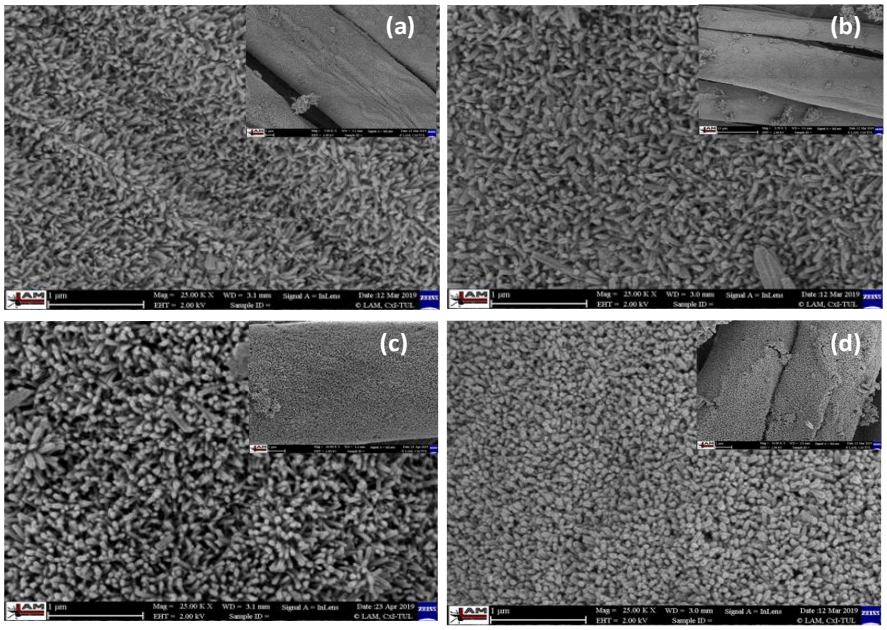

Figure 27. SEM images of ZnO nanorods grown onto cotton fabric in microwave reactor at 360 W (60 %) for 10 min under various concentration of zinc nitrate hexahydrate/HMTA: (a) 25 mM, (b) 50 mM, (c) 75 mM, and (d) 100 mM. Insets are the corresponding low magnification images

Figure 28 shows the SEM images of the nanorods grown on the ZnO seeded cotton fibers after microwave hydrothermal reaction at different reaction time. The as-prepared ZnO nanorods were

well faceted, with the diameter of 35–54 nm and an axial length of 190–295 nm under different reaction time (Figure 28). The length (L) and diameter (D) was increased with increase in reaction time. For instance, length and diameter increases from 190 nm to 295 nm and 35 nm to 54 nm respectively, when the reaction time increases from 10 min to 30 min. Therefore, the reaction time is also an important factor to control the size of the nanorods [74], [75].

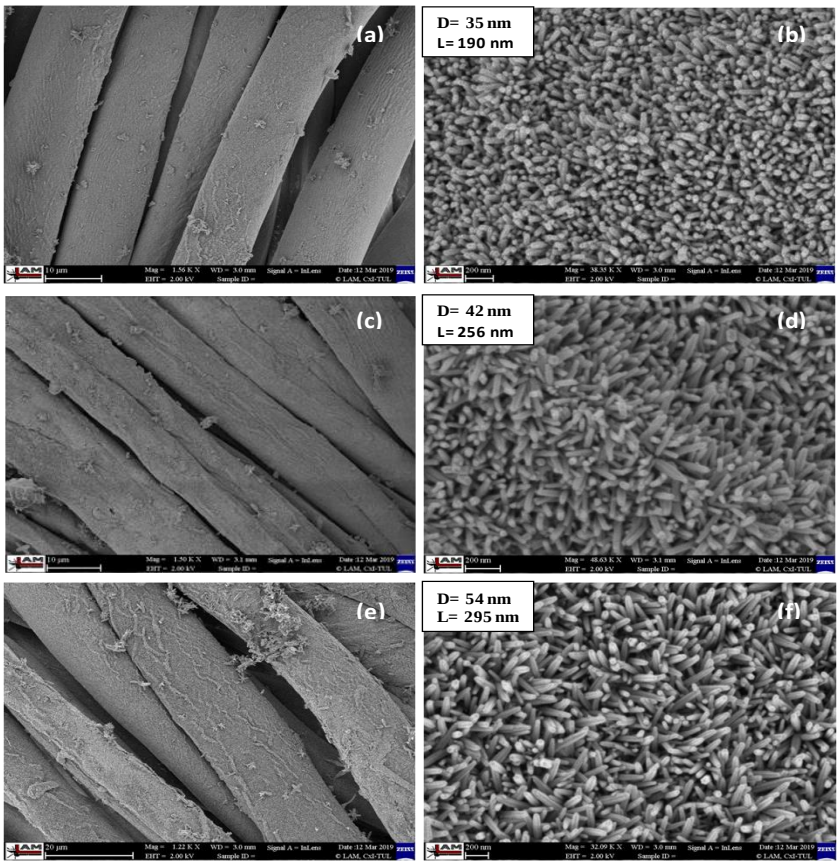

Figure 28. SEM images of ZnO nanorods grown on cotton surfaces treated with 25 mM of Zinc nitrate hexahydrate/HMTA in microwave reactor at 360 W (60 %) for different reaction time: (a, b) 10 min, (c, d) 20 min and (e, f) 30 min

The effect of microwave power on the growth rate of nanorods was also studied. The microwave power was found to have great influence on both the axial and lateral growth rates of the nanorods. The microwave power level was found to be proportional to the growth rate of the nanorods. This is mainly due to the rapid heating of the precursors to its crystallization temperature and quick dissolution of the precipitated hydroxides [76]. It was observed that longer and thicker nanorods can be obtained at higher microwave power levels.

Figure 29(a–f) shows the SEM images of as-grown nanorods at different microwave power levels (360 W, 420 W and 480 W) for 10 min. A homogenous and continuous film of ZnO nanorods can be seen on cotton fiber surface. The nanorods grown at high microwave power (480 W) had higher diameter (44 nm) and length (308 nm) as compared to nanorods grown at 360 W and 420 W of microwave powers (Figure 29e, f). The nanorods having averaged diameter of 40 nm and length of 270 nm were grown at microwave power of 420 W (Figure 29c, d). The increase in microwave power causes the rapid heating of the solution simultaneously, which enhance the nucleation and

growth of the ZnO crystal [77], [78]. Thus, rapid growth of longer and thicker nanorods can be achieved by increasing the microwave power. It can be concluded that microwave powers has great influence on enhancing the dimensions of the nanorods. The above discussion indicated that ZnO nanorods film can be successfully prepared on the cotton fibers. The size and morphology of the as-prepared nanorods can be controlled by changing salt concentrations, reaction time and microwave power levels. Therefore, we can conclude that an increase in the concentration of zinc nitrate hexahydrate/HMTA induces the changes in the kinetics of nucleation and growth, which may results in a change of size and density of the ZnO nanorods on the fiber surfaces.

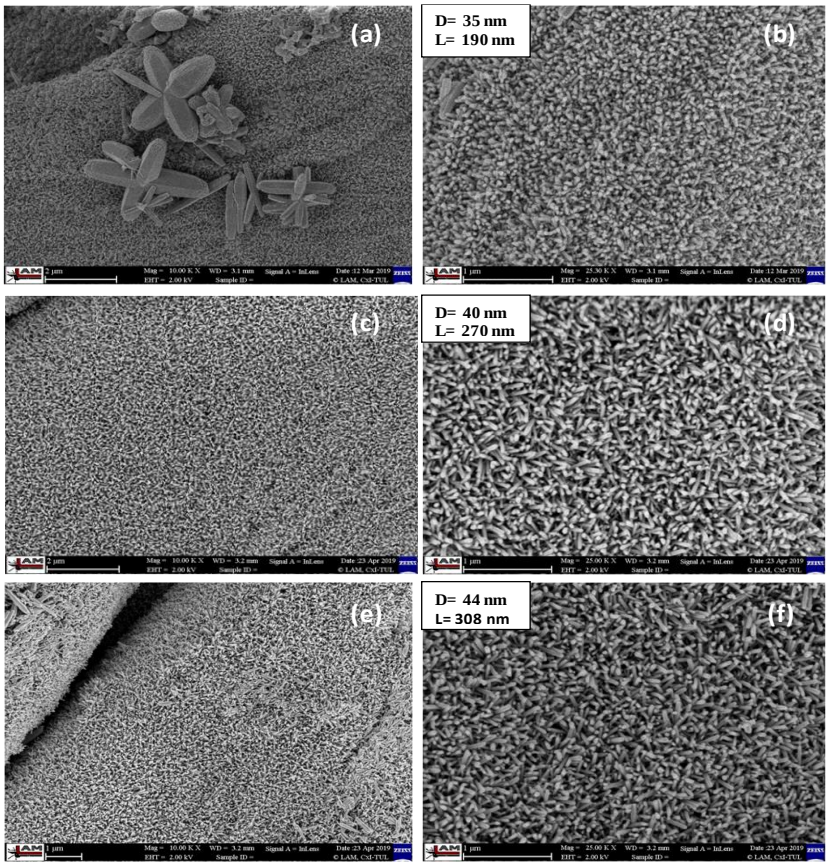

Figure 29. SEM images of ZnO nanorods grown on cotton surfaces treated with 25 mM of Zinc nitrate hexahydrate/HMTA in microwave reactor for 10 min at different microwave powers (watt): (a, b) 360 W (60 %) , (c, d) 420 W (70 %) and (e, f) 480 W (80 %)

5.3.2. EDS analysis

To confirm the composition of these as-grown nanorods, the samples were investigated by energy disperse spectroscopy (EDS). The EDS analysis clearly showed that these uniformly distributed nanorods were mainly composed of Zn and O elements (Figure 30). Samples treated with various concentration of zinc nitrate hexahydrate showed almost similar amount of Zn content as shown in Table 3. Additionally, the amount of Zn content on the different coated fabrics can be attributed to the crystallinity of the grown nanorods [79]. The presence of Pt element was caused by sputtering of platinum on ZnO coated sample during SEM characterization.

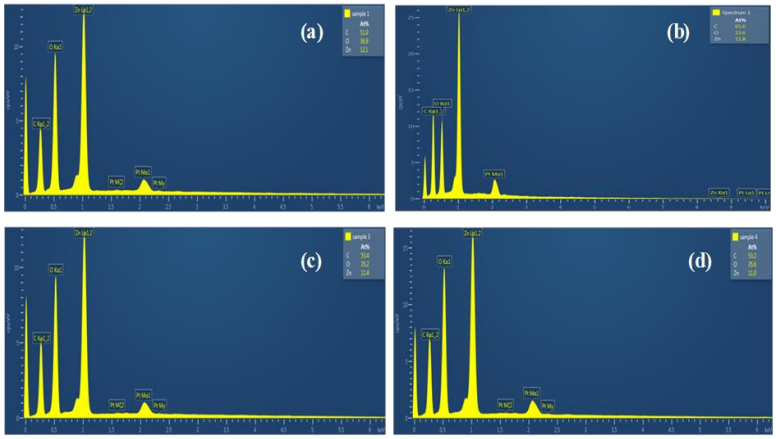

Figure 30. EDS spectra of ZnO nanorods coated cotton fabrics at various concentration of Zinc nitrate hexahydrate/HMTA for 10 min: (a) 25 mM, (b) 50 mM, (c) 75 mM, and (d) 100 mM

Table 3. Elemental composition of ZnO nanorods coated cotton fabrics

Element (wt. %)	Sample treated with 25 mM	Sample treated with 50 mM	Sample treated with 75 mM	Sample treated with 100 mM
C	30.71	41.09	32.88	33.11
O	29.57	18.86	28.88	29.65
Zn	39.73	40.05	38.24	37.25

5.3.3. XRD analysis

The ZnO nanorods coated cotton fabric samples exhibited typical diffraction peaks of ZnO at 2θ: 37.0, 40.2, 42.3, 55.8, 66.8, 74.5, 79.9, 80.9 and 82.3 which correspond to the (100), (002), (101), (102), (110), (103), (200), (112), (201) planes of ZnO (Figure 31). All the observed peaks represent the hexagonal wurtzite structure of ZnO nanorods. No extraordinary diffraction peaks were observed in the XRD patterns and three sharp peaks confirmed the presence of highly pure and crystalline nature of ZnO nanorods on the cotton fiber surfaces [70], [80].

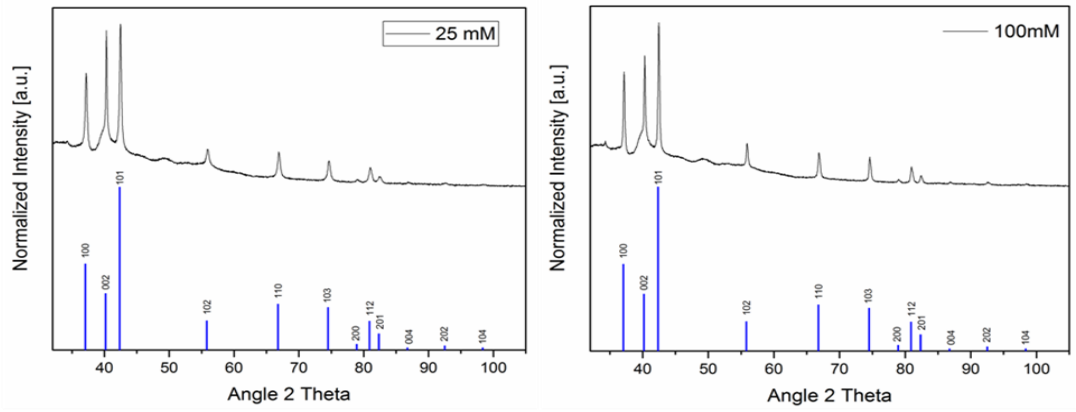

Figure 31. XRD patterns of the ZnO nanorods grown at 25 mM and 100 mM concentration of $Zn(NO_3)_2 \cdot 6H_2O$/HMTA. All peaks are indexed according to ICCD Card No. 01-083-6338

5.3.4. Topography and roughness analysis

Figure 32 shows the AFM images and surface profiles of the grown nanorods on cotton fabric surfaces at different level of concentrations (i.e., 25 mM to 100 mM). A uniform and continuous pattern of grown ZnO nanorods can be seen for all the samples. AFM analysis shows that each sample has different roughness and topographic patterns. The growth patterns and orientations of the nanorods changed due to different crystal growth under various concentration of zinc nitrate hexahydrate.

The average roughness (Ra) measured for samples treated with various concentration of zinc nitrate hexahydrate are given in Table 4. The sample coated with 25 mM of concentration exhibited minimum roughness 26.2 nm. The surface roughness of the samples was ranged from 26.2 to 61.3 nm for various concentration of zinc nitrate hexahydrate (25 mM to 100 mM). The sample coated with 100 mM of concentration shows very dense growth of nanorods due to which the tip of AFM cannot go between the nanorods hence the topography is different. The AFM images of sample coated with 25 mM showed the presence of nanorods at a certain distance from each other that allow the movement of micro tip between the nanorods. At less concentration, the distance between the consecutive nanorods increased but a uniform growth pattern was observed. While at high concentration, dense packing of nanorods was observed. The roughness is greatly influenced by the size and growth direction of the nanorods. In previous study, the average roughness was found to increase with increase of nanorods diameter [81]. It has been reported that the roughness depends on the alignment and orientation of the grown nanorods [82]. Similar amount of surface roughness were reported for ZnO nanorods grown superhydrophobic surfaces [83]. It can be concluded that morphology and size of the grown nanorods highly affect the topography and roughness of the surface.

Table 4. Analysis of surface roughness

$Zn(NO_3)_2 \cdot 6H_2O$ Concentration (mM/L)	Roughness (nm)
25	26.2 (±3.5)
50	36.6 (±2.3)
75	61.3 (±7.1)
100	45.1 (±5.2)

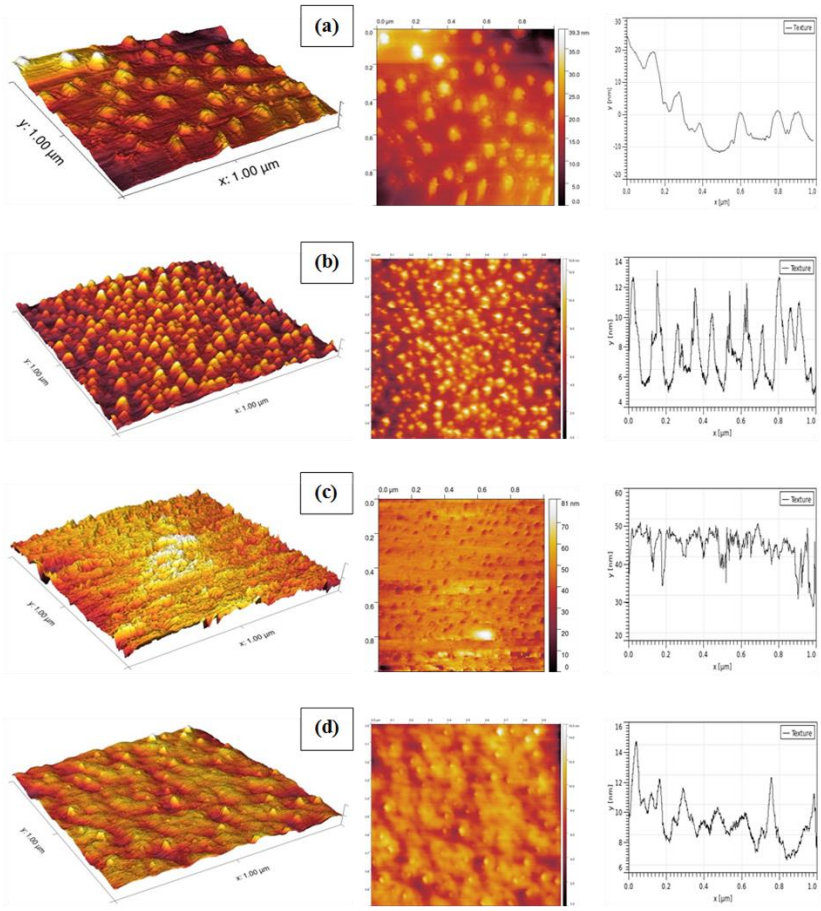

Figure 32. AFM images and surface profiles of ZnO nanorods grown fabrics at various concentration of zinc nitrate hexahydrate, (a) 25 mM, (b) 50 mM, (c) 75 mM, and (d) 100 mM

5.3.5. Superhydrophobic properties of ZnO-OTMS coated cotton fabrics

The static water contact angle and roll-off angle are the most widely used wetting measurements. These measurements were made to study the effect of zinc nitrate hexahydrate concentration on the wettability of the ZnO-OTMS coated cotton fabric (Figure 33). The pristine cotton fabric completely absorbed water droplet due to presence of hydroxyl groups in the structure. Without any deposition of ZnO nanorods and with only coating of OTMS on cotton fabric, the water contact angle and roll off-angle were measured around 130.1^{o} and 19^{o} respectively. The increase in contact angle and decrease in roll-off angle was observed, when cotton fabric surface was deposited with ZnO nanorods and subsequent treatment of OTMS. In our study, the nanorods coated surfaces were found to be superhydrophobic with WCA of greater than 150^{o}. The maximum WCA of 170.2^{o} and minimum roll off angle of 1^{o} was found for 25 mM of zinc nitrate hexahydrate concentration. The WCAs of 164.6^{o}, 161.4^{o} and 158.8^{o} were achieved for 50 mM, 75 mM, and 100 mM of concentrations, respectively. The increase of zinc nitrate hexahydrate concentration was resulted into little decrease of WCA that could be possibly due to increase in diameter and dense packing of the grown nanorods. We noted that the surface roughness in combination with the particle size is important factor for higher water contact angles. In all cases, the coated surfaces were found to be superhydrophobic. Although the sample coated with 25 mM of concentration (D=35 nm, L=190 nm) did not provide the highest surface roughness, but the size and orientation of the nanorods

enhanced the fraction of the air pocket at the composite interface which is in accordance with the Cassie-Baxter state. Therefore, optimum size of nanorods can be grown to achieve the desire superhydrophobicity. These results demonstrate that the size, shape, and orientation of the nanoparticles also play an important role when designing suitable superhydrophobic surfaces [84], [85]. Finally, the development of superhydrophobic surfaces can be achieved when cotton fiber surface is decorated with nanorods and subsequently modified with OTMS. The surface roughness produced by nanorods is responsible for the formation of lotus effect. This phenomenon can be related to the formation of unique micro/nano structural surface providing necessary roughness and improving the surface hydrophobicity.

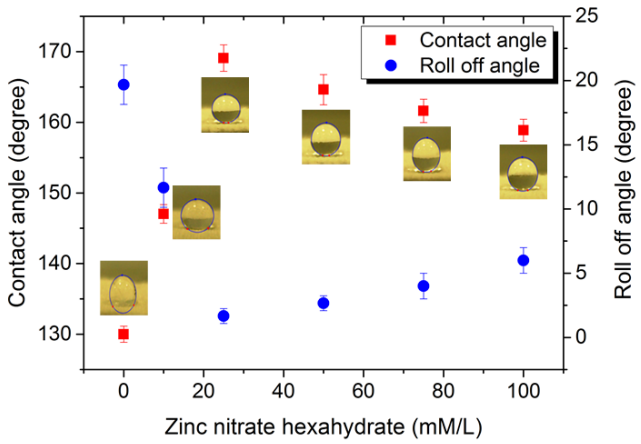

Figure 33. Effect of zinc nitrate hexahydrate concentration on water contact angle

Figure 34(a) shows that the wetted solid fraction was decreased to lowest value for 25 mM of zinc nitrate hexahydrate treated sample and further increase of concentration was resulted into slightly increase of wetted solid fraction, which could be due to increase in size and shape of ZnO nanorods. The significant increase of unwetted fraction of the air pocket was observed for the 25 mM to 100 mM of zinc nitrate hexahydrate concentration except sample treated with 10 mM of concentration. The maximum unwetted fraction of the air pocket of 95% was found for 25 mM of zinc nitrate hexahydrate. These results further confirmed that the continuous and homogenous layer of nanorods constructed a rough surface for the air storage to resist the penetration of liquid. The work of adhesion was found to reduce with increase in surface density and the change in morphology of the ZnO nanorods (see Figure 34b). The untreated cotton fabric coated with OTMS alone depicted the work of adhesion around 26.01 mN/m, whereas the work of adhesion ranged from 11.7 to 1.34 mN/m for ZnO-OTMS coated cotton fabrics at concentrations of zinc nitrate hexahydrate from 10mM to 100 mM. The fabric surface decorated with nanorods at 25 mM of zinc nitrate hexahydrate concentration exhibited least work of adhesion or smallest work required for the movement of the water drop.

The force of attraction was found to increase with increased size of ZnO nanorods on the surface of cotton fabric (Figure 34c). The cotton fabric coated with OTMS alone, the force of attraction was found around 23.22 (10^{-8}dyne/cm^2). However, the force of attraction was measured from 10.49 to 1.19 (10^{-8}dyne/cm^2) after the decoration of ZnO nanorods at various zinc nitrate hexahydrate concentrations of 10mM to 100 mM. The least force of attraction was found around 1.19 (10^{-8}dyne/cm^2) for the fabric decorated with ZnO nanorods at 25 mM of zinc nitrate hexahydrate

concentration. These results showed that less force required for movements of water drops on the fabric surface coated with ZnO nanorods and OTMS.

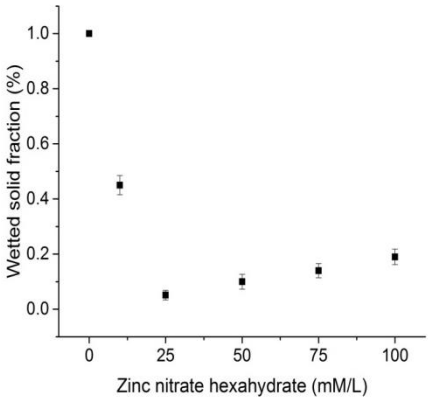

(a). Cassie-Baxter prediction

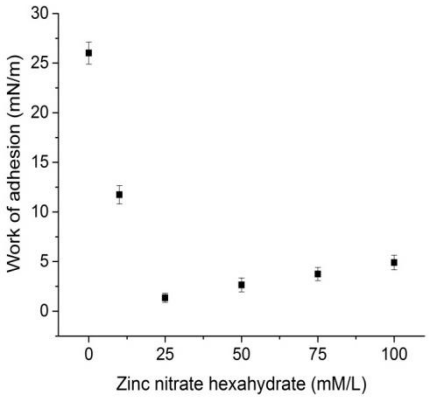

(b). Work of adhesion

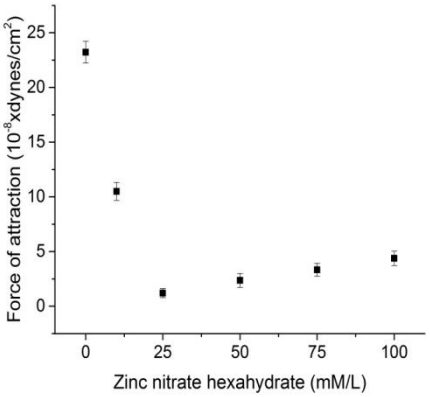

(c). Force of attraction

Figure 34. Analysis of superhydrophobicity of ZnO-OTMS coated cotton fabrics

5.3.6. Durability of ZnO-OTMS coated cotton fabrics

The durability of ZnO-OTMS coated cotton fabrics against mechanical abrasion, laundering, chemical and UV action was evaluated and contact angle results after exposure are shown in Figure 35. The contact angle of the ZnO-OTMS coated cotton fabrics was studied after 20 cycles of sand paper abrasion. All the coated samples showed reduction in water contact angle, but the WCAs were still higher than 150^{o} except sample coated with 10 mM of zinc nitrate hexahydrate. The sample coated with 25 mM of zinc nitrate hexahydrate showed greater reduction in WCA and exhibited WCA of 156.5^{o} after mechanical abrasions. The sample with 50 mM of concentration exhibited good stability after mechanical actions with a WCA of 158.4^{o}. The samples deposited with nanorods showed acceptable reduction in water contact angle after five laundering cycles. However, the sample coated with 50mM maintained highest water contact angle of 160.2^{o}. These results shows the robustness and durability of the nanorods grown samples against mechanical and friction forces [6]. It has been observed that the samples showed acceptable reduction of WCAs and retained their hydrophobicity after exposure to chemical environment. Reduction of WCA after alkali exposure was greater than acidic environment. The durability of ZnO-OTMS coated cotton fabrics against ultraviolet rays was also evaluated and it was seen that the contact angle of

the ZnO-OTMS coated fabrics was not affected after exposure to ultraviolet rays. Thus, it is suitable to use under solar irradiations.

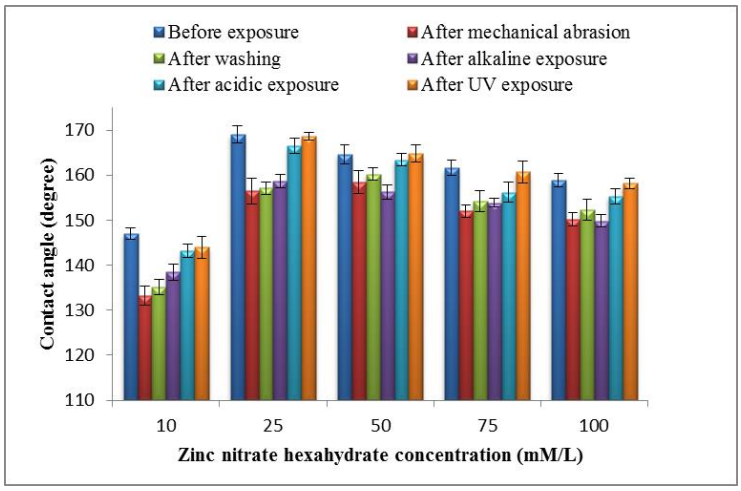

Figure 35. Durability of ZnO-OTMS coated cotton fabrics

5.3.7. Physical self-cleaning properties of ZnO-OTMS coated cotton fabrics

To demonstrate the self-cleaning property of the superhydrophobic ZnO-OTMS coated cotton fabrics methyl orange dye was used as a contaminant. The superhydrophobic fabric was fixed on a transparent glass slides that leans against a round dish with a small angle of inclination (Figure 36). When the water droplets were dropped on the contaminated fabric, it rolled over the surface and maintained the spherical shape. During the sliding process of water droplets, the dye particles were immediately picked up and taken away leaving behind a clear surface. Digital images were obtained at different moment. This behavior was attributed to the creation of lotus effect by high water surface tension and low surface energy of coated fabrics [66].

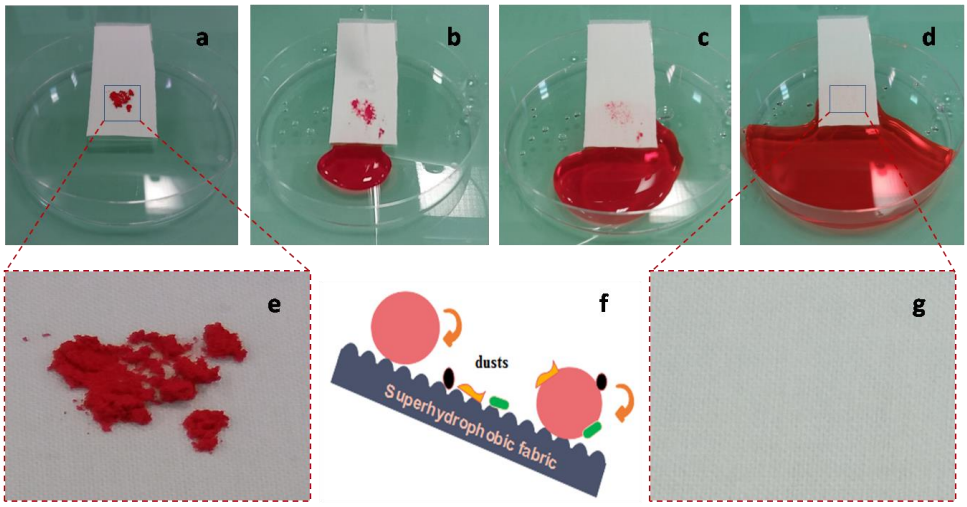

Figure 36. The self-cleaning process of ZnO-OTMS coated cotton fabric (a–d). The high magnify optical images of ZnO-OTMS coated cotton fabric before self-cleaning (e), and after self-cleaning (g), and corresponding schematic illustration of the self-cleaning process (f)

6. Evaluation of results and new findings

6.1. Conclusions

The following conclusions have been drawn from each study.

In first study, fly ash particles were utilized to create superhydrophobic and UV protective cotton fabrics. The surface of fly ash was mechanically activated by ball milling process. The unmilled fly ash with particle diameter of 3547 nm was converted to smaller particles of below 1000 nm diameter after 30 min dry pulverization. The milled fly ash particles were then coated on cotton fabric surfaces at 1, 2 and 3 wt% concentration. Due to presence of hydroxyl groups, the fly ash particles showed better adhesion with cotton fiber surfaces. When the utility of fly ash coated fabrics was investigated for UV protection properties, maximum UV blocking was observed in case of cotton fabric coated with 3 wt% fly ash. The untreated cotton fabric showed a low UPF of 9.49, however all the cotton fabrics decorated with fly ash particles exhibited large increase in UPF values due to their high refractive index and presence of metal oxide constituents. The topography of fly ash coated cotton fabric was characterized using AFM and surface roughness was found to increase with increase in fly ash concentration. In order to achieve superhydrophobic properties, the non-fluorinated silane was applied on previous fly ash coated fabrics. The water contact angle was measured around 130^{o} for coated fabrics of OTMS alone. However, when fly ash concentration of 1, 2 and 3 wt % was applied; the contact angle was improved to 143^{o}, 147^{o} and 153^{o}, respectively. The enhancement in water repellency was attributed to the formation of unique two-tier structural surface combined with the microscaled cotton fibers and the nanoscaled fly ash particles. Based on Cassie-Baxter theories, 43%, 55% and 67% increase in the unwetted fraction of the air pocket trapped in the interspaces among the fly ash particles was estimated for 1, 2 and 3 wt% of fly ash particles respectively. Further, 14.58 to 8.28 mN/m ranges for work of adhesion and 13.13 to 7.45 dyne/cm^2 ranges for force of attraction were estimated with increased density of fly ash coating. When the utility of fly ash-OTMS coated cotton fabrics was investigated for oil in water separation performance, 98%, 96%, 97% and 95% of separation efficiency was obtained for toluene/water, n-hexane/water, chloroform/water and petro ether/water, respectively. This showed the ability of fly ash coated fabrics for versatile separation of oil/water mixtures under various conditions (e.g. floating oil layer, underwater oil droplet or oil/water mixtures).

In second study, the amount of TTIP was found to have a great effect on the growth and structure of TiO_2 nanoflowers. The assembly of TiO_2 particles in flower shape was not found at low dose of TTIP. However, the amount and the size of TiO_2 flower structures were greatly increased by further increase in TTIP dose from 1 mL to 2.0 mL. The maximum roughness value (Ra) of 78.8 nm was calculated for the flower-like TiO_2 nanoparticles coated polyester. The increase in contact angle and reduction in roll of angle was observed with the increase of TTIP dose, where maximum static contact angle of 160.1^{o} and minimum roll off angle of 3^{o} was found for 2 mL TTIP dose. Furthermore, the formation of discontinuous, unstable, and contorted air/solid/liquid contact line was found as the contact angle hysteresis reduced from 9° to 3° with increase in TTIP dose. From Cassie–Baxter state superhydrophobicity, 58%, 78% and 83% increase in unwetted fraction of the air pocket was calculated for 1 mL, 1.5 mL and 2 mL TTIP dose respectively. Moreover, the reduction in work of adhesion (11.4 to 4.34 mN/m) and force of attraction (10.27 to 3.9 10^{-8}dyne/cm^2) indicated less force required for movements of water drops on the polyester fabric surface decorated with more number of TiO_2 flowers. The surface of TiO_2-OTMS coated polyester fibers also showed the promising results to maintain the superhydrophobic durability against

mechanical abrasion, laundering, chemical and UV action. When the coated fabrics were examined for physical self-cleaning, the methyl orange dye particles were immediately picked up and taken away by the rolling water droplets. The coated fabrics also exhibited the chemical self-cleaning action as the stains of methyl orange dye disappeared mostly within 3 h and the samples became approximately white after 4 h.

In third study, a novel microwave hydrothermal method was used to grow aligned ZnO nanorods on cotton fabrics. It was found that the salt concentration, reaction time and microwave irradiation power have great effect on the size and growth of ZnO nanorods. The growth of ZnO nanorods were not found at 10 mM of zinc nitrate hexahydrate. However, the growth and the size of ZnO nanorods were greatly increased by increase in zinc nitrate hexahydrate concentration from 25mM to 100 mM. Similarly, size of ZnO nanorods was increased when reaction time and microwave power was increased from 10 min to 30 min and 360 W to 480 W, respectively. Moreover, the non-fluorinated silane (OTMS) was applied on the ZnO nanorods coated fabrics to incorporate superhydrophobic properties. The AFM analysis showed that the nano-roughness changed with the change in concentration of zinc nitrate hexahydrate. The maximum water contact angle of 170.2^{o} and minimum roll off angle of 1^{o} was found for 25 mM of zinc nitrate hexahydrate concentration. The slight decrease in contact angle and increase in roll of angle was observed with the increase of zinc nitrate hexahydrate concentration. Furthermore, from Cassie–Baxter state the maximum unwetted fraction of the air pocket of 95% was found for 25 mM of zinc nitrate hexahydrate. Moreover, the reduction in work of adhesion and force of attraction also indicated less force required for movements of water drops on the ZnO nanorods and OTMS coated fabric. The ZnO-OTMS coated cotton fabrics also showed the promising results to maintain the superhydrophobic durability against mechanical abrasion, laundering, chemical and UV action. The methyl orange dye was quickly picked up by rolling water droplets during physical self-cleaning of the ZnO-OTMS coated cotton fabrics. The ZnO-OTMS coated cotton fabrics also showed great oil/water separation performance when investigated for mixture of chloroform/water, n-hexane/water, petro ether/water and toluene/water, respectively.

6.2. Future work

- In future, durable superhydrophobic surfaces can be developed through single step approach by using fly ash, TiO_2 and ZnO particles.
- Further investigations are needed in future on precisely controlling surface roughness and structure in both small and large scales.
- New theoretical model also needs to be developed apart from Cassie and Wenzel to gain deep insight regarding the mechanism of superhydrophobicity.
- More work is needed to investigate how to enhance the durability of superhydrophobic surfaces.
- The future trend is to develop durable self-healing superhydrophobic surfaces that can automatically restore original characteristics after having been damaged.

7. References

[1] V. Pandiyarasan, S. Suhasini, J. Archana, M. Navaneethan, A. Majumdar, Y. Hayakawa, and H. Ikeda, "Fabrication of hierarchical ZnO nanostructures on cotton fabric for wearable device applications," *Appl. Surf. Sci.*, vol. 418, pp. 352–361, 2017.

[2] N. Valipour M., F. C. Birjandi, and J. Sargolzaei, "Super-non-wettable surfaces: A review," *Colloids Surfaces A Physicochem. Eng. Asp.*, vol. 448, no. 1, pp. 93–106, 2014.

[3] M. Zhang and C. Wang, "Fabrication of cotton fabric with superhydrophobicity and flame retardancy," *Carbohydr. Polym.*, vol. 96, no. 2, pp. 396–402, 2013.

[4] A. Esfandiari, "PPy covered cellulosic and protein fibres using novel covering methods to improve the electrical property," *World Appl. Sci. J.*, vol. 3, no. 3, pp. 470–475, 2008.

[5] M.-E. Y. Amirhossein Esfandiari, Hossein Nazokdast, AboSaeed Rashidi, "Review of Polymer-Organoclay Nanocomposites," *J. Appl. Sci.*, vol. 8, no. 3, pp. 545–561, 2008.

[6] S. Li, J. Huang, M. Ge, C. Cao, S. Deng, S. Zhang, G. Chen, K. Zhang, S. S. Al-Deyab, and Y. Lai, "Robust Flower-Like TiO_2@Cotton Fabrics with Special Wettability for Effective Self-Cleaning and Versatile Oil/Water Separation," *Adv. Mater. Interfaces*, vol. 2, no. 14, p. 1500220, 2015.

[7] Z. Du, C. Cheng, L. Tan, J. Lan, S. Jiang, L. Zhao, and R. Guo, "Enhanced photocatalytic activity of Bi2WO6/TiO2composite coated polyester fabric under visible light irradiation," *Appl. Surf. Sci.*, vol. 435, pp. 626–634, 2018.

[8] M. Z. Khan, V. Baheti, J. Militky, A. Ali, and M. Vikova, "Superhydrophobicity, UV protection and oil/water separation properties of fly ash/Trimethoxy(octadecyl)silane coated cotton fabrics," *Carbohydr. Polym.*, vol. 202, no. August, pp. 571–580, 2018.

[9] M. Z. Khan, V. Baheti, M. Ashraf, T. Hussain, A. Ali, A. Javid, and A. Rehman, "Development of UV Protective, Superhydrophobic and Antibacterial Textiles Using ZnO and TiO_2 Nanoparticles," *Fibers Polym.*, vol. 19, no. 8, pp. 1647–1654, 2018.

[10] L. Yao and J. He, "Recent progress in antireflection and self-cleaning technology - From surface engineering to functional surfaces," *Prog. Mater. Sci.*, vol. 61, pp. 94–143, 2014.

[11] S. Afzal, W. A. Daoud, and S. J. Langford, "Superhydrophobic and photocatalytic self-cleaning cotton," *J. Mater. Chem. A*, vol. 2, no. 42, pp. 18005–18011, 2014.

[12] W. Barthlott and C. Neinhuis, "Purity of the sacred lotus, or escape from contamination in biological surfaces," *Planta*, vol. 202, no. 1, pp. 1–8, 1997.

[13] S. Li, J. Huang, Z. Chen, G. Chen, and Y. Lai, "A review on special wettability textiles: theoretical models, fabrication technologies and multifunctional applications," *J. Mater. Chem. A*, vol. 5, no. 1, pp. 31–55, 2017.

[14] H. Song, T. Chen, Y. L. Sun, X. Q. Zhang, and X. H. Jia, "Controlled synthesis of porous flower-like TiO_2 nanostructure with enhanced photocatalytic activity," *Ceram. Int.*, vol. 40, no. 7 PART B, pp. 11015–11022, 2014.

[15] A. M. Rather, N. Jana, S. Begum, H. K. Srivastava, and U. Manna, "Exceptional control on physical properties of a polymeric material through alcoholic solvent-mediated environment-friendly Michael addition reaction," *Green Chem.*, vol. 19, no. 19, pp. 4527–4532, 2017.

[16] J. Ju, X. Yao, X. Hou, Q. Liu, Y. S. Zhang, and A. Khademhosseini, "A highly stretchable and robust non-fluorinated superhydrophobic surface," *J. Mater. Chem. A*, vol. 5, no. 31, pp. 16273–16280, 2017.

[17] M. Zhang, J. Li, D. Zang, Y. Lu, Z. Gao, J. Shi, and C. Wang, "Preparation and

characterization of cotton fabric with potential use in UV resistance and oil reclaim," *Carbohydr. Polym.*, vol. 137, pp. 264–270, 2016.
[18] A. Panda, P. Varshney, S. S. Mohapatra, and A. Kumar, "Development of liquid repellent coating on cotton fabric by simple binary silanization with excellent self-cleaning and oil-water separation properties," *Carbohydr. Polym.*, vol. 181, no. November 2017, pp. 1052–1060, 2018.
[19] G. Broasca, G. Borcia, N. Dumitrascu, and N. Vrinceanu, "Characterization of ZnO coated polyester fabrics for UV protection," *Appl. Surf. Sci.*, vol. 279, pp. 272–278, 2013.
[20] B. Xu, J. Ding, L. Feng, Y. Ding, F. Ge, and Z. Cai, "Self-cleaning cotton fabrics via combination of photocatalytic TiO2and superhydrophobic SiO2," *Surf. Coatings Technol.*, vol. 262, pp. 70–76, 2015.
[21] B. Bhushan and Y. C. Jung, "Natural and biomimetic artificial surfaces for superhydrophobicity, self-cleaning, low adhesion, and drag reduction," *Prog. Mater. Sci.*, vol. 56, no. 1, pp. 1–108, 2011.
[22] L. Zou, C. Lan, X. Li, S. Zhang, Y. Qiu, and Y. Ma, "Superhydrophobization of cotton fabric with multiwalled carbon nanotubes for durable electromagnetic interference shielding," *Fibers Polym.*, vol. 16, no. 10, pp. 2158–2164, 2015.
[23] Z. H. Zhang, H. J. Wang, Y. H. Liang, X. J. Li, L. Q. Ren, Z. Q. Cui, and C. Luo, "One-step fabrication of robust superhydrophobic and superoleophilic surfaces with self-cleaning and oil/water separation function," *Sci. Rep.*, vol. 8, no. 1, pp. 1–12, 2018.
[24] Y. Lu, S. Sathasivam, J. Song, C. R. Crick, C. J. Carmalt, and I. P. Parkin, "Robust self-cleaning surfaces that function when exposed to either air or oil," *Science (80-.).*, vol. 347, no. 6226, pp. 1132–1135, 2015.
[25] S. S. Latthe and A. V. Rao, "Superhydrophobic SiO_2 micro-particle coatings by spray method," *Surf. Coatings Technol.*, vol. 207, pp. 489–492, 2012.
[26] M. Z. Khan, M. Ashraf, T. Hussain, A. Rehman, M. M. Malik, Z. A. Raza, Y. Nawab, and Q. Zia, "In situ Deposition of TiO_2 Nanoparticles on Polyester Fabric and Study of Its Functional Properties," *Fibers Polym.*, vol. 16, no. 5, pp. 1092–1097, 2015.
[27] C.-H. Xue, S.-T. Jia, H.-Z. Chen, and M. Wang, "Superhydrophobic cotton fabrics prepared by sol–gel coating of TiO_2 and surface hydrophobization," *Sci. Technol. Adv. Mater.*, vol. 9, no. 3, p. 035001, Jul. 2008.
[28] C. Te Hsieh, F. L. Wu, and S. Y. Yang, "Superhydrophobicity from composite nano/microstructures: Carbon fabrics coated with silica nanoparticles," *Surf. Coatings Technol.*, vol. 202, no. 24, pp. 6103–6108, 2008.
[29] Y. Wang, Z. Mo, C. Zhang, P. Zhang, R. Guo, H. Gou, R. Hu, and X. Wei, "Morphology-controllable 3D flower-like TiO_2 for UV shielding application," *J. Ind. Eng. Chem.*, vol. 32, pp. 172–177, 2015.
[30] J. Wang, F. Han, and S. Zhang, "Durably superhydrophobic textile based on fly ash coating for oil/water separation and selective oil removal from water," *Sep. Purif. Technol.*, vol. 164, pp. 138–145, 2016.
[31] S. Faheem, V. Baheti, M. Tunak, J. Wiener, and J. Militky, "Comparative performance of flame retardancy, physiological comfort, and durability of cotton textiles treated with alkaline and acidic casein suspension," *J. Ind. Text.*, p. 152808371775088, 2017.
[32] A. Das, J. Deka, A. M. Rather, B. K. Bhunia, P. P. Saikia, B. B. Mandal, K. Raidongia, and U. Manna, "Strategic Formulation of Graphene Oxide Sheets for Flexible Monoliths and Robust Polymeric Coatings Embedded with Durable Bioinspired Wettability †," *ACS Appl.*

Mater. Interfaces, vol. 9, no. 48, pp. 42354–42365, 2017.
[33] D. Parbat, S. Gaffar, A. M. Rather, A. Gupta, and U. Manna, "A general and facile chemical avenue for the controlled and extreme regulation of water wettability in air and oil wettability under water," *Chem. Sci.*, vol. 8, no. 9, pp. 6542–6554, 2017.
[34] A. M. Rather and U. Manna, "Stretchable and durable superhydrophobicity that acts both in air and under oil," *J. Mater. Chem. A*, vol. 5, no. 29, pp. 15208–15216, 2017.
[35] X. N. Tang, A. E. Berman, R. A. Swanson, and M. A. Yenari s, "Digitally quantifying cerebral hemorrhage using Photoshop®and Image J," *J. Neurosci. Methods*, vol. 190, no. 2, pp. 240–243, 2010.
[36] V. Baheti, J. Militky, R. Mishra, and B. K. Behera, "Thermomechanical properties of glass fabric/epoxy composites filled with fly ash," *Compos. Part B Eng.*, vol. 85, pp. 268–276, Feb. 2015.
[37] P. Cataldi, I. S. Bayer, R. Cingolani, S. Marras, R. Chellali, and A. Athanassiou, "A Thermochromic Superhydrophobic Surface," *Sci. Rep.*, vol. 6, no. February, pp. 1–11, 2016.
[38] X. Dong, S. Gao, J. Huang, S. Li, T. Zhu, Y. Cheng, Y. Zhao, Z. Chen, and Y. Lai, "A self-roughened and biodegradable superhydrophobic coating with UV shielding, solar-induced self-healing and versatile oil-water separation ability," *J. Mater. Chem. A*, vol. 7, no. 5, pp. 2122–2128, 2019.
[39] X. Luo, Y. Weng, S. Wang, J. Du, H. Wang, and C. Xu, "Superhydrophobic and oleophobic textiles with hierarchical micro-nano structure constructed by sol–gel method," *J. Sol-Gel Sci. Technol.*, vol. 89, no. 3, pp. 820–829, 2019.
[40] H. R. Pant, M. P. Bajgai, K. T. Nam, Y. A. Seo, D. R. Pandeya, S. T. Hong, and H. Y. Kim, "Electrospun nylon-6 spider-net like nanofiber mat containing TiO_2 nanoparticles: A multifunctional nanocomposite textile material," *J. Hazard. Mater.*, vol. 185, no. 1, pp. 124–130, 2011.
[41] C. Pan, L. Shen, S. Shang, and Y. Xing, "Preparation of superhydrophobic and UV blocking cotton fabric via sol-gel method and self-assembly," *Appl. Surf. Sci.*, vol. 259, pp. 110–117, 2012.
[42] Y. Zhao, Z. Xu, X. Wang, and T. Lin, "Superhydrophobic and UV-blocking cotton fabrics prepared by layer-by-layer assembly of organic UV absorber intercalated layered double hydroxides," *Appl. Surf. Sci.*, vol. 286, pp. 364–370, 2013.
[43] A. Ali, V. Baheti, J. Militky, and Z. Khan, "Utility of silver-coated fabrics as electrodes in electrotherapy applications," *J. Appl. Polym. Sci.*, vol. 135, no. 23, 2018.
[44] A. Ali, V. Baheti, J. Militky, Z. Khan, V. Tunakova, and S. Naeem, "Copper coated multifunctional cotton fabrics," *J. Ind. Text.*, vol. 0, no. 00, p. 152808371773207, 2017.
[45] A. Ali, N. H. A. Nguyen, V. Baheti, M. Ashraf, J. Militky, T. Mansoor, M. T. Noman, and S. Ahmad, "Electrical conductivity and physiological comfort of silver coated cotton fabrics," *J. Text. Inst.*, vol. 109, no. 5, pp. 620–628, 2018.
[46] B. Xu and Z. Cai, "Fabrication of a superhydrophobic ZnO nanorod array film on cotton fabrics via a wet chemical route and hydrophobic modification," *Appl. Surf. Sci.*, vol. 254, no. 18, pp. 5899–5904, 2008.
[47] Y. Zhao, Y. Tang, X. Wang, and T. Lin, "Superhydrophobic cotton fabric fabricated by electrostatic assembly of silica nanoparticles and its remarkable buoyancy," *Appl. Surf. Sci.*, vol. 256, no. 22, pp. 6736–6742, 2010.
[48] P. Aminayi and N. Abidi, "Ultra-oleophobic cotton fabric prepared using molecular and nanoparticle vapor deposition methods," *Surf. Coatings Technol.*, vol. 276, pp. 636–644,

2015.
[49] M. Ashraf, C. Campagne, A. Perwuelz, P. Champagne, A. Leriche, and C. Courtois, “Development of superhydrophilic and superhydrophobic polyester fabric by growing Zinc Oxide nanorods,” *J. Colloid Interface Sci.*, vol. 394, no. 1, pp. 545–553, 2013.
[50] X. Zhu, Z. Zhang, B. Ge, X. Men, X. Zhou, and Q. Xue, “A versatile approach to produce superhydrophobic materials used for oil-water separation,” *J. Colloid Interface Sci.*, vol. 432, pp. 105–108, 2014.
[51] B. Jiang, Z. Chen, Y. Sun, H. Yang, H. Zhang, H. Dou, and L. Zhang, “Fabrication of superhydrophobic cotton fabrics using crosslinking polymerization method,” *Appl. Surf. Sci.*, vol. 441, pp. 554–563, 2018.
[52] P. Aminayi and N. Abidi, “Imparting super hydro/oleophobic properties to cotton fabric by means of molecular and nanoparticles vapor deposition methods,” *Appl. Surf. Sci.*, vol. 287, pp. 223–231, 2013.
[53] J. Wang, G. Geng, A. Wang, X. Liu, J. Du, Z. Zou, S. Zhang, and F. Han, “Double biomimetic fabrication of robustly superhydrophobic cotton fiber and its application in oil spill cleanup,” *Ind. Crops Prod.*, vol. 77, pp. 36–43, 2015.
[54] F. Liu, M. Ma, D. Zang, Z. Gao, and C. Wang, “Fabrication of superhydrophobic/superoleophilic cotton for application in the field of water/oil separation,” *Carbohydr. Polym.*, vol. 103, no. 1, pp. 480–487, 2014.
[55] Y. Jin, P. Jiang, Q. Ke, F. Cheng, Y. Zhu, and Y. Zhang, “Superhydrophobic and superoleophilic polydimethylsiloxane-coated cotton for oil-water separation process: An evidence of the relationship between its loading capacity and oil absorption ability,” *J. Hazard. Mater.*, vol. 300, pp. 175–181, 2015.
[56] J. Wang and G. Geng, “Highly recyclable superhydrophobic sponge suitable for the selective sorption of high viscosity oil from water,” *Mar. Pollut. Bull.*, vol. 97, no. 1–2, pp. 118–124, 2015.
[57] A. Cammarano, G. De Luca, and E. Amendola, “Surface modification and adhesion improvement of polyester films,” *Cent. Eur. J. Chem.*, vol. 11, no. 1, pp. 35–45, 2013.
[58] P. Soundarrajan, K. Sankarasubramanian, T. Logu, K. Sethuraman, and K. Ramamurthi, “Growth of rutile TiO_2 nanorods on TiO_2 seed layer prepared using facile low cost chemical methods,” *Mater. Lett.*, vol. 116, pp. 191–194, 2014.
[59] G. Nagaraju, K. Manjunath, T. N. Ravishankar, B. S. Ravikumar, H. Nagabhushan, G. Ebeling, and J. Dupont, “Ionic liquid-assisted hydrothermal synthesis of TiO_2 nanoparticles and its application in photocatalysis,” *J. Mater. Sci.*, vol. 48, no. 24, pp. 8420–8426, Aug. 2013.
[60] X. Gan, X. Gao, J. Qiu, P. He, X. Li, and X. Xiao, “TiO_2 nanorod-derived synthesis of upstanding hexagonal kassite nanosheet arrays: An intermediate route to novel nanoporous TiO_2 nanosheet arrays,” *Cryst. Growth Des.*, vol. 12, no. 1, pp. 289–296, 2012.
[61] M. R. Subramaniam, S. Devanathan, and D. Kumaresan, “Synthesis of micrometer-sized hierarchical rutile TiO_2 flowers and their application in dye sensitized solar cells,” *RSC Adv.*, vol. 4, no. 69, pp. 36791–36799, 2014.
[62] A. M. Selman, Z. Hassan, and M. Husham, “Structural and photoluminescence studies of rutile TiO_2 nanorods prepared by chemical bath deposition method on Si substrates at different pH values,” *Meas. J. Int. Meas. Confed.*, vol. 56, pp. 155–162, 2014.
[63] N. Li, Q. Zhang, J. B. Joo, Z. Lu, M. Dahl, Y. Gan, and Y. Yin, “Water-assisted crystallization of mesoporous anatase TiO_2 nanospheres,” *Nanoscale*, vol. 8, no. 17, pp.

9113–9117, 2016.
[64] M. Li, Y. Jiang, R. Ding, D. Song, H. Yu, and Z. Chen, “Hydrothermal Synthesis of Anatase TiO2 Nanoflowers on a Nanobelt Framework for Photocatalytic Applications,” *J. Electron. Mater.*, vol. 42, no. 6, pp. 1290–1296, 2013.
[65] R. . Spurr and H. Myers, “Quantitative Analysis of Anatase-Rutile Mixtures with an X-Ray Diffractometer,” *Anal. Chem.*, vol. 29, no. 5, pp. 760–762, 1957.
[66] J. Y. Huang, S. H. Li, M. Z. Ge, L. N. Wang, T. L. Xing, G. Q. Chen, X. F. Liu, S. S. Al-Deyab, K. Q. Zhang, T. Chen, and Y. K. Lai, “Robust superhydrophobic TiO_2@fabrics for UV shielding, self-cleaning and oil-water separation,” *J. Mater. Chem. A*, vol. 3, no. 6, pp. 2825–2832, 2015.
[67] F. Xu, Y. Lu, Y. Xie, and Y. Liu, “Controllable morphology evolution of electrodeposited ZnO nano/micro-scale structures in aqueous solution,” *Mater. Des.*, vol. 30, no. 5, pp. 1704–1711, 2009.
[68] R. Nandi and S. S. Major, “The mechanism of growth of ZnO nanorods by reactive sputtering,” *Appl. Surf. Sci.*, vol. 399, pp. 305–312, 2017.
[69] M. Skompska and K. Zarębska, “Electrodeposition of ZnO nanorod arrays on transparent conducting substrates-a review,” *Electrochim. Acta*, vol. 127, pp. 467–488, 2014.
[70] M. He, W. Li, J. Ran, D. Cheng, J. Wu, G. Cai, and X. Wang, “Hydrothermal growing of cluster-like ZnO nanoparticles without crystal seeding on PET films via dopamine anchor,” *Appl. Surf. Sci.*, vol. 467–468, no. August 2018, pp. 534–542, 2018.
[71] V. R. Shinde, T. P. Gujar, T. Noda, D. Fujita, A. Vinu, M. Grandcolas, and J. Ye, “Growth of shape- and size-selective zinc oxide nanorods by a microwave-assisted chemical bath deposition method: Effect on photocatalysis properties,” *Chem. - A Eur. J.*, vol. 16, no. 34, pp. 10569–10575, 2010.
[72] K. Edalati, A. Shakiba, J. Vahdati-Khaki, and S. M. Zebarjad, “Low-temperature hydrothermal synthesis of ZnO nanorods: Effects of zinc salt concentration, various solvents and alkaline mineralizers,” *Mater. Res. Bull.*, vol. 74, pp. 374–379, 2016.
[73] H. Zhang, D. Yang, X. Ma, N. Du, J. Wu, and D. Que, “Straight and thin ZnO nanorods: Hectogram-scale synthesis at low temperature and cathodoluminescence,” *J. Phys. Chem. B*, vol. 110, no. 2, pp. 827–830, 2006.
[74] R. Wahab, Y. S. Kim, K. Lee, and H. S. Shin, “Fabrication and growth mechanism of hexagonal zinc oxide nanorods via solution process,” *J. Mater. Sci.*, vol. 45, no. 11, pp. 2967–2973, 2010.
[75] D. Polsongkram, P. Chamninok, S. Pukird, L. Chow, O. Lupan, G. Chai, H. Khallaf, S. Park, and A. Schulte, “Effect of synthesis conditions on the growth of ZnO nanorods via hydrothermal method,” *Phys. B Condens. Matter*, vol. 403, no. 19–20, pp. 3713–3717, 2008.
[76] H. E. Unalan, P. Hiralal, N. Rupesinghe, S. Dalal, W. I. Milne, and G. A. J. Amaratunga, “Rapid synthesis of aligned zinc oxide nanowires,” *Nanotechnology*, vol. 19, no. 25, 2008.
[77] A. Ul Hassan Sarwar Rana, M. Kang, and H. S. Kim, “Microwave-assisted Facile and Ultrafast Growth of ZnO Nanostructures and Proposition of Alternative Microwave-assisted Methods to Address Growth Stoppage,” *Sci. Rep.*, vol. 6, no. April, pp. 1–13, 2016.
[78] S. Brahma, K. J. Rao, and S. Shivashankar, “Rapid growth of nanotubes and nanorods of würtzite ZnO through microwave-irradiation of a metalorganic complex of zinc and a surfactant in solution,” *Bull. Mater. Sci.*, vol. 33, no. 2, pp. 89–95, 2010.
[79] M. Küçük and M. L. Öveçoğlu, “Fabrication of SiO2–ZnO NP/ZnO NR hybrid coated

cotton fabrics: the effect of ZnO NR growth time on structural and UV protection characteristics," *Cellulose*, vol. 2, pp. 1773–1793, 2019.
[80] E. S. Ates and H. E. Unalan, "Zinc oxide nanowire enhanced multifunctional coatings for cotton fabrics," *Thin Solid Films*, vol. 520, no. 14, pp. 4658–4661, 2012.
[81] H. Ghayour, H. R. Rezaie, S. Mirdamadi, and A. A. Nourbakhsh, "The effect of seed layer thickness on alignment and morphology of ZnO nanorods," *Vacuum*, vol. 86, no. 1, pp. 101–105, 2011.
[82] T. Dedova, I. O. Acik, M. Krunks, V. Mikli, O. Volobujeva, and A. Mere, "Effect of substrate morphology on the nucleation and growth of ZnO nanorods prepared by spray pyrolysis," *Thin Solid Films*, vol. 520, no. 14, pp. 4650–4653, 2012.
[83] G. Qi, H. Zhang, and Z. Yuan, "Superhydrophobic brocades modified with aligned ZnO nanorods," *Appl. Surf. Sci.*, vol. 258, no. 2, pp. 662–667, 2011.
[84] D. Hill, H. Attia, A. R. Barron, and S. Alexander, "Size and morphology dependent surface wetting based on hydrocarbon functionalized nanoparticles," *J. Colloid Interface Sci.*, vol. 543, pp. 328–334, 2019.
[85] R. G. Karunakaran, C. Lu, Z. Zhang, and S. Yang, "Highly Transparent Superhydrophobic Surfaces from the Coassembly of Nanoparticles (e 100 nm)," *Langmuir*, vol. 27, pp. 4594–4602, 2011.

8. List of papers published by the author

8.1. Publications in impact factor journals

1. **Muhammad Zaman Khan**, Vijay Baheti, Jiri Militky, Azam Ali, and Martina Vikova. "Superhydrophobicity, UV-protection and oil/water separation properties of fly ash/trimethoxy (octadecyl) silane coated cotton fabrics." *Carbohydrate Polymers* 202 (2018): 571-580. **(Impact factor = 7.18)**
2. **Muhammad Zaman Khan**, Jiri Militky, Vijay Baheti, Mateusz Fijalkowski, Jakub Wiener, Lukáš Voleský, and Kinga Adach. "Growth of ZnO nanorods on cotton fabrics via microwave hydrothermal method: effect of size and shape of nanorods on superhydrophobic and UV-blocking properties." *Cellulose* 27, no. 17 (2020): 10519-10539. **(Impact factor = 4.21)**
3. **Muhammad Zaman Khan**, Vijay Baheti, Jiri Militky, Jakub Wiener, and Azam Ali. "Self-cleaning properties of polyester fabrics coated with flower-like TiO2 particles and trimethoxy (octadecyl) silane." *Journal of Industrial Textiles* 50, no. 4 (2020): 543-565. **(Impact factor = 2.01)**
4. **Muhammad Zaman Khan**, Jiri Militky, Vijay Baheti, Jakub Wiener, and Michal Vik. "Development of durable superhydrophobic and UV protective cotton fabric via TiO2/trimethoxy (octadecyl) silane nanocomposite coating." *The Journal of The Textile Institute* (2020): 1-12. **(Impact factor = 1.23)**
5. **Muhammad Zaman Khan**, Vijay Baheti, Munir Ashraf, Tanveer Hussain and Azam Ali. "Development of UV Protective, Superhydrophobic and Antibacterial Textiles Using ZnO and TiO_2 Nanoparticles.*" Fibers and Polymers* 19, no. 8 (2018): 1647-1654. **(Impact factor = 1.79)**
6. **Muhammad Zaman Khan**, Sajid Hussain, Faisal Siddique, Vijay Baheti, Jiri Militky "Improvement of liquid moisture management in plaited knitted fabrics". *TEKSTİL VE KONFEKSİYON* 28, (2018): 182-188. **(Impact factor = 0.27)**

7. **Muhammad Zaman Khan**, Munir Ashraf, Tanveer Hussain, Abdur Rehman, Muhammad Mohsin Malik, and Qasim Zia. "In situ deposition of TiO_2 nanoparticles on polyester fabric and study of its functional properties." *Fibers and Polymers* 16, no. 5 (2015): 1092-1097. **(Impact factor = 1.79)**
8. Ali, Azam, Vijay Baheti, **Muhammad Zaman Khan**, Munir Ashraf, and Jiri Militky. "Development of electrically conductive composites based on recycled resources." The *Journal of the Textile Institute* 111, no. 1 (2020): 16-25. **(Impact factor = 1.23)**
9. Ali, Azam, Vijay Baheti, Jiri Militky, **Zaman Khan**, and Guocheng Zhu. "Metal Coating on Ultrafine Polyester Non-woven Fabrics and Their Ageing Properties." *Fibers and Polymers* 20, no. 7 (2019): 1347-1359. **(Impact factor = 1.79)**
10. Ali, Azam, Vijay Baheti, Jiri Militky, and **Zaman Khan**. "Utility of silver-coated fabrics as electrodes in electrotherapy applications." *Journal of Applied Polymer Science* 135, no. 23 (2018): 46357. **(Impact factor = 2.52)**
11. Azam Ali, Vijay Baheti, Jiri Militky, **Zaman Khan**, and Syed Qummer Zia Gilani. "Comparative Performance of Copper and Silver Coated Stretchable Fabrics." *Fibers and Polymers* 19, no. 3 (2018): 607-619. **(Impact factor = 1.79)**
12. Azam Ali, Vijay Baheti, Jiri Militky, **Zaman Khan**, Veronika Tunakova, and Salman Naeem. "Copper coated multifunctional cotton fabrics." *Journal of Industrial Textiles* 48, no. 2 (2018): 448-464. **(Impact factor = 2.01)**
13. Azeem, Musaddaq, Jakub Wiener, and **Muhammad Zaman Khan**. "Hydrophobic analysis of nano-filament polyester fabric.'' *Vlakna a Textil*, 2018.
14. Hussain, Sajid, Viera Glombikova, Antonín Havelka, Hafsa Jamshaid, Syeda Sidra Batool, **Muhammad Zaman Khan**. "MOISTURE TRANSPORT PHENOMENA OF FUNCTIONAL." *Vlakna a Textil*, 2017.
15. **Muhammad Zaman Khan**, Jiri Militky, Jakub Wiener "Development of multi-functional cotton fabrics by microwave hydrothermal synthesis of zinc oxide nanorods" Under Submission.

8.2. Publications in international conferences

1. **Muhammad Zaman Khan**, Jiri Militky, Jakub Wiener, "Enhanced Disinfection of Titanium Dioxide" Textile Bioengineering and Informatics Symposium (TBIS) 2020, Webinar, July 2020.
2. **Muhammad Zaman Khan**, Vijay Baheti, Jiri Militky, "Superhydrophobicity, UV protection and oil/water separation properties of TiO_2 nanoparticles and Trimethoxy(octadecyl)silane coated cotton fabrics" The Fiber Society Fall 2019 Conference*:* University of Texas, Austin, USA, October 2019.
3. **Muhammad Zaman Khan**, Vijay Baheti, Jiri Militky, "Development of Superhydrophobic Cotton Fabrics and Their Functional Properties" ICDTC 2019 : 21th International Conference on Defence Textiles and Clothing, London, United Kingdom, June 2019.
4. **Muhammad Zaman Khan**, Vijay Baheti, Jiri Militky, "Self-cleaning polyester fabrics decorated with flower like TiO_2 particles" CEC 2019: 10th Central European Conference, Lodz, Poland, October 2019.
5. **Muhammad Zaman Khan**, Vijay Baheti, Jiri Militky, "Hydrothermal synthesis of TiO_2 nanoparticles on PET fabric and their functional properties" The 47^{th} Textile Research Symposium, Liberec, Czech Republic, June 2019.

6. **Muhammad Zaman Khan**, Vijay Baheti, Jiri Militky, "Development of multifunctional polyester fabric functionalized with TiO_2 nanoparticles" 18th World Textile Conference (AUTEX), Istanbul, Turkey, June 2018.
7. **Muhammad Zaman Khan**, Vijay Baheti, Jiri Militky, "Superhydrophobization of cotton fabric with fly ash for durable UV protection and oil/water separation properties." International PhD Students Day, 22nd Strutex 2018, Liberec, Czech Republic.
8. **Muhammad Zaman Khan**, Vijay Baheti, Jiri Militky,"Study the functional properties of polyester fabric functionalized with TiO_2 nanoparticles." 195th International Conference on Innovative Engineering Technologies (ICIET). Rawalpindi: IRES, 2017.
9. Musaddaq Azeem, Jakub Wiener, and **Muhammad Zaman Khan**. "Hydrophobic treatment of nano-filament polyester fabric.'' International Ph.D. Students Day. CEC 2017, Liberec, Czech Republic.

8.3. Publications in book chapters

1. **Muhammad Zaman Khan**, Jiri Militky, Jakub Wiener, Azam Ali, "Titanium Dioxide: - Enhanced Disinfection" Textiles and Their Use in Microbial Protection: Focus on COVID-19 and Other Viruses, 1st edition, CRC Press, ISBN 9780367691059, June 2021.
2. **Muhammad Zaman Khan**, Vijay Baheti, Jiri Militky, "Methods for characterization and evaluation of self-cleaning textiles" Recent Trends in Fibrous Material Science, Vol- 5, September 2019.
3. Azam Ali, Jiri Militky, **Muhammad Zaman Khan**, "Impact of copper and ions against coronavirus" Textiles and Their Use in Microbial Protection: Focus on COVID-19 and Other Viruses, 1st edition, CRC Press, ISBN 9780367691059, June 2021.
4. Ahmed Hassanin, Yuanfeng Wang, **Muhammad Zaman Khan**, Vijay Baheti, Jiri Militky, "Surface modification of textile fibers by whiskerization" Recent Trends in Fibrous Material Science, Vol- 5, September 2019.

8.4. Research projects

1. Leader of the student grant competition (SGS) project 2019, titled, "Conventional and microwave-assisted hydrothermal methods for coating of textiles", Faculty of Textile Engineering, Technical University of Liberec, Czech Republic.

2. Leader of the student grant competition (SGS) project 2018, titled, "Superhydrophobic textiles with added functionality", Faculty of Textile Engineering, Technical University of Liberec, Czech Republic.

3. Member of the student grant competition (SGS) project 2017, titled, "Preparation of modified carbon sorbents", Faculty of Textile Engineering, Technical University of Liberec, Czech Republic.

8.5. Citations

Article: Muhammad Zaman Khan, Vijay Baheti, Jiri Militky, Azam Ali, and Martina Vikova. "Superhydrophobicity, UV-protection and oil/water separation properties of fly ash/trimethoxy (octadecyl) silane coated cotton fabrics." *Carbohydrate Polymers* 202 (2018): 571-580. **(Impact factor = 7.18)**

- Cited in 21 articles.

Article: Muhammad Zaman Khan, Vijay Baheti, Munir Ashraf, Tanveer Hussain and Azam Ali. "Development of UV Protective, Superhydrophobic and Antibacterial Textiles Using ZnO and TiO_2 Nanoparticles. *" Fibers and Polymers* 19, no. 8 (2018): 1647-1654. **(Impact factor = 1.79)**

- Cited in 15 articles

Article: Muhammad Zaman Khan, Vijay Baheti, Jiri Militky, Jakub Wiener, and Azam Ali. "Self-cleaning properties of polyester fabrics coated with flower-like TiO2 particles and trimethoxy (octadecyl) silane." *Journal of Industrial Textiles* 50, no. 4 (2020): 543-565. **(Impact factor = 2.01)**

- Cited in 4 articles

Article: Muhammad Zaman Khan, Jiri Militky, Vijay Baheti, Jakub Wiener, and Michal Vik. "Development of durable superhydrophobic and UV protective cotton fabric via TiO2/trimethoxy (octadecyl) silane nanocomposite coating." *The Journal of The Textile Institute* (2020): 1-12. **(Impact factor = 1.23)**

- Cited in 1 article

9. Curriculum Vitae

Muhammad Zaman Khan

Address	Jestedska 341/103, Dolni Hanychov, 46008 Liberec, Czech Republic
Nationality	Pakistani
Date of Birth	2 January, 1990
Contacts	Mobile: 00420774357781 Email: zamankhan017@yahoo.com

Education	**Ph.D. in Textile Technics and Materials Engineering (2015 - Present)** Technical University of Liberec, Czech Republic **M.Sc. Textile Engineering (2012 - 2014)** National Textile University, Faisalabad, Pakistan **B.Sc. Textile Engineering (2006 - 2010)** The University of Faisalabad, Faisalabad, Pakistan Major: Textile chemistry
Work Experience	**Visiting Lecturer (2014 - 2015)** National Textile University Faisalabad, Pakistan **Officer (2011 - 2013)** Research and Development Department MASOOD Textile Mills Faisalabad, Pakistan
Languages	English, Urdu and Punjabi
Competencies and skills	OriginLab, MiniTAB, MS Office, MS Excel, Chem Window, Photoshop, Edraw Max and Comsol Multiphysics

Awards and Honors

- Outstanding presentation award, Textile Bioengineering and Informatics Symposium (TBIS) 2020.
- Best poster award, International PhD Students Day 2019, Technical University of Liberec, Czech Republic.

Recommendation of the supervisor

Supervisor´s opinion on PhD Thesis of Mr. Muhammad Zaman Khan, M.Sc.

Mr. Muhammad Zaman Khan, M.Sc. has worked for this PhD thesis since 2015.

The PhD thesis of Mr. Muhammad Zaman Khan, M.Sc. is titled „FUNCTIONAL PROPERTIES OF SUPERHYDROPHOBIC TEXTILES“. Field of his PhD study is “Textile Technics and Materials Engineering”.

This dissertation is focused on the development of superhydrophobic surfaces by inexpensive, simple techniques with added functionalities (i.e. UV protection, Self-cleaning) by deposition of fly ash, TiO_2 and ZnO particles. This work is formally divided to 3 studies according used chemicals and technologies. The main advantage of this PhD work is the application of high level nanotechnologies on textile structures.

Mr. Muhammad Zaman Khan has done his work systematically and on required scientific level. The language of the thesis is good and meets the PhD standard.

The publication activities are at excellent level. He published 12 papers in impacted journals, 4 books chapters and lot of papers published at conferences. In majority of these papers is Mr. Muhammad Zaman Khan a first author. Published papers are focused on surface modification, wettability and electrical properties of textiles, these orientation is in right relationship with the topic of his PhD thesis. Published papers are cited.

Mr. Muhammad Zaman Khan is an excellent PhD. Student.

I therefore recommend the thesis for defense.

prof. Ing. Jakub Wiener, PhD.
supervisor

Opponent's reviews

Opponent's review

Title: Functional properties of superhydrophobic textiles

Author: Muhammad Zaman Khan

The presented thesis deals with the study of final treatments of textile materials, which contain a synthesis of a highly hydrophobic textile fabric surface and its subsequent use in the field of self-cleaning and separation of non-polar solvents from water.

Thesis contains 121 pages divided into 6 main chapters and contains 10 tables and 59 pictures.

Research in this thesis is divided into 2 separate branches and 6 goals are set. The first branch is the use of fly ash on a cotton substrate, the second direction of research is use of the hydrothermal method to positively influence the growth of inorganic oxide nanoparticles on a textile substrate in order to create a superhydrophobic surface. Two inorganic oxides are chosen, TiO_2 and ZnO. Silane-based compound (OTMS) are also used to create a surface with the required properties.

The first and second chapters contains concise description of superhydrophobic effect and individual goals is defined.

The following chapter contains a literature search of current knowledge in the field of superhydrophobic textile materials with a focus on self-cleaning textiles and use of fly ah, TiO_2 and ZnO. Author do not forget to describe the individual models, which evaluate this treatment. Next part of this chapter is devoted to description of selected published articles focused on the use of the above-mentioned chemical compounds based on silane in combination with inorganic oxides TiO_2 and ZnO.

> I have no significant comments on the above chapters, the chapters are written clearly and with a logical sequence.

The fourth chapter contains the procedures used for surface preparation, whether the use of fly ash on cotton fabric, including the subsequent preparation of a superhydrophobic surface by OTMS, or the use of hydrothermal process in the formation of nanorods of TiO_2, respectively. ZnO for polyester, resp. cotton fabric and subsequent reactions with OTMS. The study of the superhydrophobic surface is performed using standard instrumental analytical methods, AFM or SEM. Quantitative analysis is subsequently performed by EDS, study of Raman spectra and X-Ray diffraction. Finally, the useful properties of the textiles prepared in this way are evaluated by measuring UV protection, as well as determining the contact and roll off angles and the self-cleaning and separation effect. The author does not forget to test the stability of these treatments in different environments, either at different pH or after mechanical dry and wet effect.

> The individual procedures are described in sufficient detail and the methods of evaluation of the prepared superhydrophobic surfaces are chosen appropriately. When author used the standard deviation for individual measurements, I miss the mention of how many measured values it is calculated. I would also recommend writing to the following chemical formula of zinc nitrate: $Zn(NO_3)_2 . 6H_2O$.

In the first part of the results, the doctoral student deals with the preparation of the superhydrophobic surface of a cotton substrate by fly ash. The UV protection of the cotton surface with fly ash and then the above-mentioned characteristics of the hydrophobic surface formed in combination with OTMS

were monitored. The limit of superhydrophobic and mainly self-cleaning properties is reached with 3 wt. fly ash.

The second part of the results deals with the characterization of TiO2 nanorods on a polyester substrate. The presence and distribution of inorganic oxide on the surface of the fibers has been sufficiently demonstrated. The superhydrophobic properties of the fabric prepared in this way have been proven since 1.5 mL of Titanium isopropoxide. The generally known photocatalytic behavior of TiO_2 is studied on to photocatalytically degradation selected azo dye.

The results of the use of ZnO are described in more detail in this thesis, especially concerning the characterization of the resulting nanorods. In contrast to the previous results, the optimization of the hydrothermal process for the preparation of nanorods, on which these results are based, is described here. The superhydrophobic properties achieve best results compared with TiO_2 or fly ash. The possibility of oil / water system separation was subsequently investigated.

Formally, the work is written at a very good language level with a minimum of typing errors. Graphic objects are readable and follow the previous text. I have two comments on the formal page of this thesis:

p. 43 Fig. 26, it would be better to use the same scale in all cases to compare individual SEM images

It ill be better to divide pictures to more captions. The content of this caption should not be divided at the end of the page

My comments on formal part of this thesis do not reduce the quality of the submitted work.

The thesis presents interesting results of experimental work in the field of super hydrophobic systems. The doctoral student demonstrated systematic scientific work. According to the attached list of publications, he also published his results sufficiently (co-author of 12 already published articles, 5 times of them as the main author, co- author of 8 papers at international conferences and 2 chapters in a book). I also appreciate the proposal for the future direction of further research.

My questions:

1. In the graph 25a, p. 41 it is evident that the ground ash has a Max distribution curve in the value of milled fly ash is about 2000 nm in the graph 25a, p. 41, but in the text it is written the size of the part less than 1000 nm (in the graph these sizes are almost zero). Explain this discrepancy.
2. Which %wt of fly ash is used for AFM analysis?
3. How do you explain the ratio of individual elements in a 50 ml sample of ZnO relative to the other concentrations (Table 9, p. 84)?

In conclusion, **I recommend** this thesis for the defense.

In Pardubice on December 2, 2020 **Ing. Michal Černý, Ph.D.**

Referee´s report on PhD. thesis of

Muhammad Zaman Khan

„ Functional properties of Superhydrophobic Textiles“

Professor Miroslav Černík

The presented thesis consists of 120 pages divided into 6 chapters. The thesis is based on 3 separate topics connected by a principle in a surface modification to get a hydrophobic and self-cleaning surface. The thesis has standard parts - Aims and objectives, Literature review, Research methodology, Results and discussions, and Conclusions and future work. In the end, there are References and a List of author´s publications. The author´s list of publications is extensive.

Abstract

The author made here an introduction to his work and explained the objectives of the study. It is the development of superhydrophobic surfaces by inexpensive, eco-friendly and straightforward techniques with added functionality. He selected fly ash and titanium and zinc oxides, but there is no explanation why these were particularly selected. He then describes three studies for each of the surface modifiers, but what I am missing here (and at the Conclusions as well) is comparing these three methods to each other. The presented thesis looks like three individual works (papers) on the same topic but without connection to make it one solid piece of work.

Chapter 1

introduces the work, where superhydrophobic natural structures and a short history of man-made developments are shown.

Chapter 2

deals with the aims and objectives of the thesis. The prepared modified fabrics have the common aim of increasing their hydrophobicity; moreover, the other properties were aimed, mainly, e.g., UV-blocking, antibacterial properties, flame-retardant, anti-fogging, oil/water separation. In the present thesis, UV protection, self-cleaning, and oil/water separations.

Chapter 3

deals with literature review. There is a sufficient number of literature sources, but the structure of the chapter is slightly chaotic. Some of the parts should be discussed in more detail, and some, which have no significant influence on the results, should be shortened. Some literature sources are also missing (e.g., the first equation- de Broglie, author? Source?). Some errors are here as well (e.g., "…negative electrons and oxygen combined into $O_2^{-"}$; it is superoxide radical (anion)).

Chapter 4

is about the methodology. It describes materials, fabrics coating with three different methods, and various methods of surface characterization. In general, the chapter consists of all methods applied, but some of the descriptions are relatively short without sufficient details (e.g., for roughness determined by AFM it is mentioned "software calculates the surface roughness").

Chapter 5
is about the results. There is a lot of excellent results for all three methods of surface modifications. In all cases, the results show improvement of desired properties of the fabrics. As I wrote already in the Abstract part, a comparison of these three results would significantly improve the work's unification.

Chapter 6
The chapter summarizes the major conclusions of the work. There are the following. The addition of fly ash caused significant improvement of hydrophobicity and UV protection of the surface. Due to the metal content in the ash, the UPF increased by two orders of magnitude. Also, organic/water separation efficiency for toluene, n-hexane, chloroform and ether were higher than 95%.

The addition of titanium dioxide creates nanoflowers. These structures appeared significantly at the dose of 2 ml. The contact angle was increased, and hysteresis decreased. The modified surface also showed promising results to maintain durability against mechanical abrasion, laundering, and chemical and UV action. The surface also exhibited self-cleaning by the degradation of methyl orange.

In the last part, the microwave hydrothermal method was used to grow ZnO nanorods. Additionally, OTMS was applied to incorporate superhydrophobic properties. The determined values of water contact angle and roll-off angle were extreme (170.2° and 1°). The modified fabrics also showed promising results to maintain their durability against mechanical abrasion, laundering, chemical and UV action, and outstanding oil/water separation performance.

Referee remarks, question and conclusions

QUESTIONS

1. You speak about TiO_2, but photoactivity is connected with only one crystalline structure (anatase). Chemical self-cleaning does not work for the other forms. Are you sure your structures are photoactive? Why in Fig.44, the surfaces of coated polyester fabrics prepared at increasing concentration of TiO_2 has more orange color?
2. Table 9 shows the elemental composition of ZnO nanorods. Why is there a drop in oxygen percentage for 50 mM? It does not correspond with Zn content.
3. Could you make a simple (in table) comparison of all three methods of surface functionalization? Just + and – for selected properties and 3 materials.

Imperfections and recommendations
The thesis is written in perfect English with a minimum of typing errors.

Referee´s conclusion
The presented thesis of M.Z. Khan is logical, has all the necessary parts, and shows the author understands his work. He can make appropriate preparation of the coated fabrics and their characteristics, and put his results into logical and appropriate conclusions. The thesis shows one subject with three various views (surface modifications). The work significantly contributes to knowledge in the subject. There are only a few recommendations for the next author´s work. The language is perfect and entirely understandable.

The thesis is good and meets all criteria to be taken to the defense.

In Liberec (Czech R.) on February 6, 2021 **Professor Miroslav Černík**